JOHANNES KEPLER
UNIVERSITÄT LINZ
Netzwerk für Forschung, Lehre und Praxis

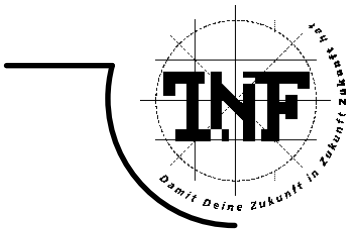

Nested Iteration Strategies for 2D elastic-plastic problems

DIPLOMARBEIT

zur Erlangung des akademischen Grades

DIPLOMINGENIEURIN

in der Studienrichtung

TECHNISCHE MATHEMATIK

Angefertigt am *Institut für Numerische Mathematik*

Betreuung:

O.Univ.Prof. Dipl.Ing. Dr. Ulrich Langer

Eingereicht von:

Birgit Rauchenschwandtner

Linz, Oktober

Zusammenfassung

Diese Diplomarbeit beschäftigt sich mit der Entwicklung von effizienten numerischen Methoden zur Simulation von elastoplastischen Modellen der Festkörper- und Strukturmechanik. Es werden nicht nur die mechanische Feldgrößen wie Verschiebungen, Verzerrungen und Spannungen berechnet, sondern auch die Entwicklung der plastischen Zonen unter den verschieden Beladungsfällen betrachtet. Diese plastischen Zonen sind vor allem in der Praxis von großer Bedeutung.
Der Einfachheit halber werden nur zweidimensionale elastoplastische Modelle mit isotroper Verfestigung betrachtet, die sich aud dem ebenen Spannungszustand und dem ebenen Verzerrungszustand ergeben.
Die Zeitdiskretisierung erfolgt mittels dem impliziten Euler Schema und die Ortsdiskretisierung mit linearen finiten Elementen in den jeweiligen hierarchischen Netzen. Wir betrachten dabei in jedem Zeitschritt das gleiche Basisgitter wobei sich durch mehrere automatisch generierte Verfeinerungen die Gitter in den höheren Ebenen voneinander unterscheiden können.
In jedem Zeitschritt und jeder Hierarchiestufe müssen wir ein nichtlineares System von finiten Elementgleichungen lösen. Aufgrund der Nichtdifferenzierbarkeit des Systems benutzen wir zur Lösung ein newtonähnliches Verfahren, das eine gute Startnäherung benötigt. Diese Näherung für den Startwert berechnen wir mittels Extrapolation der Näherungen aus dem vorigen Zeitschritt sowie dem nächst gröberen Gitter im aktuellen Zeitschritt und im vorigen Zeitschritt. Um diesen Extrapolationsalgorithmus zu implementieren müssen angemessene Interpolationsperatoren zwischen den verschiedenen Gittern gefunden werden.
Unsere numerischen Beispiele zeigen, dass diese Extrapolationstechnik einen guten Starwert liefert und auch bei adaptiver Verfeinerung funktioniert.

Abstract

This diploma thesis is devoted to the development of efficient numerical methods for the simulation of the elastoplastic model in solid and structural mechanics. Beside the evolution of the mechanical field quantities like displacements, strains and stresses, the development of the plastic zones under different load regimes is of great practical interest. For the sake of simplicity, we only consider two–dimensional elastoplastic model with isotropic hardening arising from the state of plane stress or the state of plane strain.
The time evolution is discretized by the backward Euler scheme, whereas the spatial discretization is performed by means of linear finite elements on hierarchical meshes. We keep the same coarse mesh for all time steps respectively incremental steps, but we can use different finer meshes produced by some automatic mesh adaption procedure from one time step to the next one. At each time step and at each nested mesh we have to solve a non-linear system of finite element equations. Due to the non-differentiability the finite element system is solved by a Quasi-Newton method with a suitable initial guess. A good initial guess can be obtained by extrapolation from the former time step and from the coarser mesh at the current and the former time step. In order to handle this extrapolation process, suitable transfer operators have to be defined. Our numerical experiments show that this extrapolation technique can accelerate the solution procedure even on adaptively produced meshes.

Contents

Chapter 1

Introduction, Preliminaries and Notation

1.1 Introduction

This thesis is dealing with the problem of elastoplastic deformations which occur by applying volume forces and/or surface tractions to a body. If the loads are small enough only elastic deformation happens, but by increasing the applied load also plastic deformation may occur. The main difference is that elastic deformation vanishes if the load is removed, while plastic deformation remains.
A crucial problem is to identify the unknown interface between regions of the elastic and the plastic deformation. Since the two regions vary for different loads, it is also necessary to take a different mesh for each load to garantee highest possible accuracy with the lowest calculation complexity.
The classical model of elastic deformations is based on the balance equation of force and angular momentum, the geometrical relation between strains and displacements and material laws. For plastic deformation the model is extended with a plastic flow law. This leads to a system of equation for the elastic behaviour and one inequality to describe the plastic dependency. Existence and uniqueness of the solution to the variational problem is shown in [11] for the geometrically linear case.
In [13] efficient algorithm for solving the elastoplastic problems are discussed. There the idea of time sequences and nested grids raises, which will be implemented here.
In this thesis, we will mainly concentrate on another solution algorithm

which can be found in [7]. This algorithm works with a Newton-like solver, which will also be used in this thesis.
In Section 5 we will compare our numerical results with the ones in [7]
In this work an arbitrary time dependent load is considered. In each time step a new mesh can be generated in an adaptive way starting with a fixed coarse mesh which is the same for each time step. The displacement field is calculated on different fineness levels. A further option is to do some uniform refinements before starting adaptive refinements. This structure leads to different meshes for every time step (incremental step) in which the solution is calculated.
In a typical situation the meshes are different at two different time steps i.e., there exist unique vertices in each of the meshes.

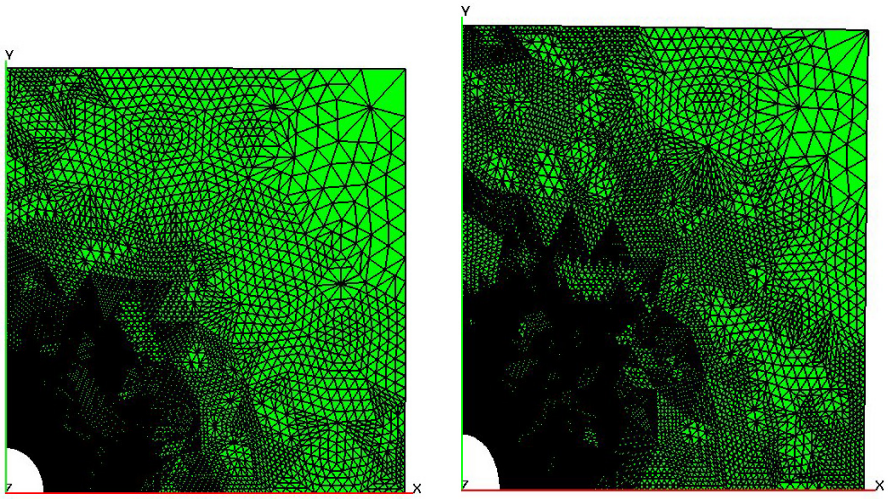

Figure 1.1: Two different adaptive meshes at the same refinement level and at different time steps resulting in different deformations of the plate with the hole.

Since the nested iteration technique is used, not only the solution on the finest mesh per time step is calculated, but rather a series of solutions on each refinement level in every time step. For such nested meshes in every time step the same coarse mesh is used.

The main advantage of building up such structures is that now an extrapolation of the starting value for the Newton-like solver can be used. It is generally known that a Newton-like method converges only locally quadratically or superlinear. However the quality of a Newton-like method is intrinsically depending on the choice of a proper initial value. As it is shown in [14] for nested grids, under some stronger assumptions (regularized elastoplastic model and H^2-regularity) the iteration number do not depend neither on the number of refinement levels nor on the time step width. For that reason the solution can be calculated very fast in higher levels and every time step. We only have to calculate once all levels in the first time step and calculate the solution on every coarse mesh.

These thesis is organized as follows:

- The following section gives a short introduction to the notations, the used function spaces and the basic instruments of convex analysis which will be used in the following chapters.
- Chapter 2 provides the mathematical modelling, first the elastic model and then the elastoplastic model with hardening. In these thesis isotropic hardening is assumed.
  Also the time discretization is done to get the minimization problem which can be solved by Newton-like methods.
- Space discretization as well as the implementation in Matlab is described and the extrapolation of the solution is done.
- The numerical results for some test problems (plate with a hole, wrench and a L-shape domain) are presented and discussed.
- The last chapter gives a conclusion summing up all important results and provides an outlook for a further improvement of dynamic nested FEM discussed in this thesis.

1.2 Preliminaries

1.2.1 Notations

There are two different types of coordinates to describe continuum mechanics problems:

- Lagrange coordinates
- Eulerian coordinates

Lagrange coordinates consider a reference configuration and calculate everything as an image of the reference configuration.

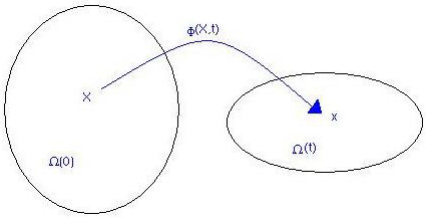

Figure 1.2: Lagrange coordinates

The Eulerian coordinates fix a space point and look which particle stays there at time t.

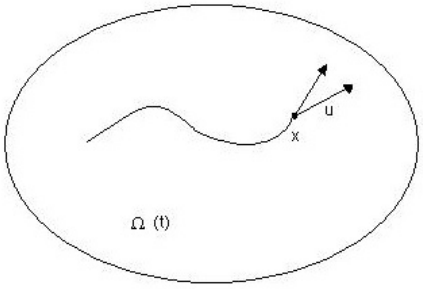

Figure 1.3: Eulerian coordinates

For elastoplastic problems the Lagrange coordinates are preferred. To distinguish between the two systems of notation all Lagrange variables are denoted by capital letters, while Eulerian variables are denoted by small letters.

The acceleration in Eulerian coordinates $a(x,t)$ describes the time change of velocity of a fixed particle which is at time t in the space point x. For the calculation of the acceleration, the derivative of the velocity $v(\Phi(X,t),t)$ with respect to t has to be build, where $v = \frac{\partial u}{\partial t}(x,t)$.

Definition 1.1 *(Material derivative)*
The differential operator $\frac{D}{Dt}$ is defined as follows

$$\frac{D}{Dt} = \frac{\partial}{\partial t} + v \cdot \frac{\partial}{\partial x} \tag{1.1}$$

and is called total or material derivative.

The acceleration $a(x,t)$, as it is described above, is defined by the material derivative $\frac{Dv}{Dt}$.

Theorem 1.1 *(Reynolds' transport theorem)*
Let $t \in (T_1, T_2)$, let $\omega \subset \mathbb{R}^d$ be a bounded domain. ω_t is the deformed body at time t with $\bar{\omega}_0 \subset \mathbb{R}^d$. Let v and F be continously differentable. Then $\int_{\omega_t} F(x,t)/dx$ is well-defined and continuously differentiable in an interval $(t_1, t_2) \subset (T_1, T_2)$ with $t \in (t_1, t_2)$. By (1.1) it follows

$$\begin{aligned} \frac{d}{dt}\int_{\omega_t} F(x,t)\, dx &= \int_{\omega_t} [\frac{\partial F}{\partial t}(x,t) + div(Fv)(x,t)]\, dx \\ &= \int_{\omega_t} [\frac{DF}{Dt}(x,t) + F\ div(v)(x,t)]\, dx. \end{aligned}$$

Proof: See [16] or many other books about continuum mechanics
By using the transport theorem, integration and derivative can be exchanged.

The following measurable spaces are assumed. If a Banach space B can be defined on the corresponding σ-algebra $\mathbb{A}$ (with measure μ), then we can introduce an L^p-space.

Definition 1.2 *Let $\Omega \subset \mathbb{R}^d$ be a bounded Lipschitz domain, then a space is called L^p-space by definition if*

$$L^p(\Omega) := \{v : \Omega \to \mathbb{R}^d \mid \int_\Omega \parallel v(x) \parallel^p \ d\mu(x) < \infty\}.$$

The α-th partial derivative $D^\alpha v$ is defined by

$$D^\alpha v := \frac{\partial^{|\alpha|} v}{\partial x^\alpha}$$

where $\alpha = (\alpha_1, \alpha_2, ...\alpha_n)$ denotes a multiindex and $\mid \alpha \mid = \sum_{i=1}^d \alpha_i$

Definition 1.3 *For any nonnegative integer m and $p \geq 1$ or $p = \infty$ the Sobolev space $W^{m,p}(\Omega)$ is defined by*

$W^{m,p}(\Omega) := \{v \in L^p(\Omega) \mid D^\alpha v \in L^p(\Omega)$ *for any* $\alpha \in \mathbb{Z}_+^d$ *where* $\mid \alpha \mid \leq m\}$

with the norm

$$\begin{aligned} \parallel v \parallel_{m,p,\Omega} &:= (\sum_{|\alpha| \leq m} \parallel D^\alpha v \parallel^p_{L^p(\Omega)})^{\frac{1}{p}} \text{ and} \\ \parallel v \parallel_{m,\infty,\Omega} &:= \max_{|\alpha| \leq m} \parallel D^\alpha v \parallel_{L^\infty(\Omega)} \end{aligned}$$

for $p \in [1, \infty)$ and $p = \infty$, respectively.
From the defintion we can see easily that $W^{m,0}(\Omega) = L^p(\Omega)$

Remark 1.1 *(Hilbert Spaces)*
For p=2, the Sobolev space $W^{m,p}(\Omega)$ is a Hilbert space, where the scalar(inner) product is given by

$$\langle v, w \rangle_{m.\Omega} = \int_\Omega \sum_{\alpha \leq m} \frac{\partial^{|\alpha|} v}{\partial x^\alpha} \frac{\partial^{|\alpha|} w}{\partial x^\alpha} \ dx.$$

The Hilbert space $W^{m,2}(\Omega)$ is sometimes denoted by $H^m(\Omega)$

The following notations are often needed in the next chapters:

$$\begin{aligned} \dot{\sigma} &= \frac{\partial \sigma}{\partial t} \ , \\ A : B &= \sum_{i,j=1}^n a_{ij} b_{ij} \ , \\ x_+ &= \begin{cases} x & \text{if } x \geq 0 \\ 0 & \text{if } x < 0 \end{cases} \ , \\ \delta_{ij} &= \begin{cases} 1 & \text{if i=j} \\ 0 & \text{else} \end{cases} \ . \end{aligned}$$

Definition 1.4 *(Frobenius Norm)*
For a matrix $A = \{a_{ij}\}_{i,j=1}^{d}$ the Frobenius Norm is defined by

$$\| A \|_F := \sqrt{\sum_{i,j=1}^{d} a_{i,j}^2} = \sqrt{A : A}$$

The deviator is defined as

$$\sigma^D = \sigma - \frac{1}{d} tr(\sigma) I$$

which expresses the deflection of the stress operator to a situation where only pure pressure force is applied.

1.2.2 Convex Analysis

This will only be a short and not complete introduction in convex analysis. For further details the reader is refered to [6].
First let us define the term "convex" to get a short view, which spaces and functionals are considered in that section.

Definition 1.5 *(Convexity)*
Let A be a subset of the vector space V. A is said to be convex if

$$\forall u, v \in A \qquad [u, v] := \{\lambda u + (1 - \lambda)v \mid 0 \leq \lambda \leq 1\} \in V$$

Definition 1.6 *(Convex Functions)*
Let A be a convex subset of the vector space V, and F a mapping of A into $\bar{\mathbb{R}}$. F is said be a convex function, if

$$\forall \lambda \in [0, 1] \forall u, v \in A \qquad F(\lambda u + (1 - \lambda)v) \leq \lambda F(u) + (1 - \lambda) F(v).$$

Afterwards the space $\Gamma(V)$ is often needed. Let's give a definition of this space

Definition 1.7 *Let V vector space and all affine continuous functions (see [6]) be of the type $v > L(v) + \alpha$, where L is a continuous linear functional over V and $\alpha \in \mathbb{R}$. Then the set of functions $F : V \to \bar{\mathbb{R}}$ which are the pointwise supremum of the family of continuous affine functions is denoted by $\Gamma(V)$.*

Lemma 1.1 *The following properties of $\Gamma(V)$ are equivalent*

- $F \in \Gamma(V)$
- *F is a convex l.s.c. function (see [6]) from V into $\bar{\mathbb{R}}$, and if F takes the value $-\infty$ then F is identically equal to $-\infty$*

Lemma 1.2 *(Γ-regularization)*
Let F and G be two functions mapping V into $\bar{\mathbb{R}}$. The following statements are equivalent to each other:

- *G is the pointwise supremum of the continuous affine functions everywhere less than F*
- *G is the largest minorant of F in $\Gamma(V)$. G is then called the Γ-regularization of F.*

Proof: See [6]
The following definitions are necessary to describe the two vector spaces V and V^* and the duality between them, which occurs by the application of the scalar product $\langle ., . \rangle$

Definition 1.8 *(Polar)*
If $F : V \to \bar{\mathbb{R}}$ and

$$f^*(u^*) = \sup_{u \in V} \{\langle u, u^* \rangle - F(u)\}$$

defines a function from V^* into $\bar{\mathbb{R}}$, denoted by F^* and is called the polar (or conjugated) function of F.

Lemma 1.3 *(Bipolar)*
If $F : V \to \bar{\mathbb{R}}$. Then its bipolar F^{**} is nothing else that its Γ-regularization. In particular, if $F \in \Gamma(V)$, $F^{**} = F$.

Proof: See [6]

Theorem 1.2 *(Subdifferentiability)*
Let F be a function mapping V into $\bar{\mathbb{R}}$ and F^* its polar. Then $u^* \in \partial F(u)$ if and only if:

$$F(u) + F^*(u^*) = \langle u, u^* \rangle ,$$

or equivalently written

$$\partial F(u) = \{u^* \in V^* \mid F^*(u^*) - \langle u, u^* \rangle \leq -F(u)\}. \tag{1.2}$$

Proof: See [6]
The subdifferentialbility of functionals will be used to generate a dual formulation of the problem. The set $\partial F(u)$ is convex and closed with respect to $\sigma(V, V^*)$ in V^*, where σ denotes the weak topology between V and V^* associated by the duality.

Chapter 2

Mathematic Models

2.1 Linear Elasticity Model

Let us start with an elastic model for a deformable body, this means that no irreversible deformations occur. The main goal is to calculate the displacement field u in the domain Ω. $\Phi(x,t)$ is the function which maps the particle x to the actual position at time t, in the notation of Lagrange coordinates notation. Mostly the displacement u

$$u(x,t) = \Phi(x,t) - x$$

is the point of interest and not the new position. The deformation process cannot be completly described by the displacement field. Rigid body motions do not cause deformations. They only rotate and/or translate the body. So it is necessary to distinguish between them, by a function for the strain and one for the rigid body motion. The elastic strain tensor is defined by

$$\begin{aligned} \epsilon(u) &= \frac{1}{2}(C(x) - I) \\ &= \frac{1}{2}(((I + \nabla u(x,t)^T)(I + \nabla u(x,t)) - I) \\ &= \frac{1}{2}(\nabla u(x,t)^T + \nabla u(x,t) + \nabla u(x,t)^T \nabla u(x,t)) \end{aligned}$$

where $C(x,t) = \nabla\Phi(x,t)^T \nabla\Phi(x,t)$ is the right Cauchy tensor.
In the most practical applications the gradient of the deformations $\parallel \nabla u \parallel$

are small. So the last term can be neglected and we end up with the linearized elastic strain tensor:

$$\epsilon(u) = \frac{1}{2}(\nabla u(x,t)^T + \nabla u(x,t)).$$

Next we take a look at the physical equations, which are the well-known background of the model.

2.1.1 Balance Equations

Equation of continuity

This balance equation explains that the mass inside a closed domain has to be the same at every time. This can be formulated mathematically as follows:
If ω_t is the domain at time t, ρ is the density of the material, x the position in the domain and t the time variable then the following equation holds:

$$\forall \omega_t \subset \Omega_t : \qquad \frac{d}{dt}\int_{\omega_t} \rho(x,t)\, dx = 0$$

It can be reformulated if ρ is smooth enough on the domain. While in this thesis only domains consisting of one material are considered, it is easy to show enough smoothness of ρ.
By using Theorem 1.1, the balance equation can be written as

$$\frac{d\rho}{dt}(x,t) + \rho(x,t) div\ v(x,t) = 0$$

Balance of momentum

Physics tells us that the change of the momentum has to be equal to the sum of the forces, in our case the sum of surface tractions and volume forces. Let us denote $F(\omega_t)$ as the sum of the forces $F_S(\omega_t)$ and $F_V(\omega_t)$ and remember that $\int_{\omega_t} \rho(x,t)v(x,t)$ is the momentum where $v(x,t) = \frac{d}{dt}u(x,t)$ is the velocity field. The forces are given by

$$F_S(\omega_t) = \int_{\partial\omega_t} \vec{t}(x,t,n(x,t))\, ds$$
$$F_V(\omega_t) = \int_{\omega_t} \rho(x,t) f(x,t)\, dx$$

where n is the normal vector. Hence $\vec{t}(x,t,n(x,t))$ is the tension in normal direction in the space point x and at time t. The value at the Dirichlet boundary is given by $\vec{t}(x,t,n(x,t)) = g(x)$. The specific force density in the equation above is denoted by $f(x,t)$.

Balance of Momentum

$$\frac{d}{dt}\int_{\omega_t} \rho(x,t)v(x,t)\,dx = \int_{\partial\omega_t} \vec{t}(x,t,n(x,t))\,ds + \int_{\omega_t} \rho(x,t)f(x,t)\,dx = F(\omega_t)$$

Also the **Balance of Angular Momentum** is valid

$$\frac{d}{dt}\int_{\omega_t} x \times \rho(x,t)v(x,t)\,dx = \int_{\partial\omega_t} x \times \vec{t}(x,t,n(x,t))\,ds + \int_{\omega_t} x \times \rho(x,t)f(x,t)\,dx = F(\omega_t)$$

Definition 2.1 *(Euler, Cauchy)*
*If the tension field vector $\vec{t}(x,t,n(x,t))$ exists, such that the balance of momentum and the balance of angular momentum is fulfilled and $\vec{t}(x,t,n(x,t)) = g(x)$ on the Dirichlet boundary. If t fulfil that also on every subset A of ω_t, then $\vec{t}(x,t,n)$ is called **Cauchy tension vector**.*

Theorem 2.1 *If $\vec{t}$ is a Cauchy tension vector and $\vec{t} \in C^1$ for fixed x and every n and $\vec{t} \in C$ for fixed n and every x, then*

$$\vec{t}(x,t,n(x,t) = \sigma(x,t) \cdot n(x,t)$$

where $\sigma(x,t)$ is the "Cauchy tension vector" and is additionally symmetric.

Proof: See [2]

With this knowledge the theorem of Gauss can be applied to the surface term. Using the transport theorem once more and the balance of mass for the left hand side we can rewrite the balance of momentum as follows

$$\rho(x,t)\underbrace{\frac{D}{Dt}v(x,t)}_{=a(x,t)} = \rho(x,t)f(x,t) + div\ \sigma(x,t)\ ,$$

where $a(x,t)$ denotes the acceleration of the particels, which is in the considered applications very small, so that it can be neglected. We end up with

$$F_V(x,t) = -div\ \sigma(x,t)\ .$$

That state is called "quasistatic". By the balance of angular momentum it can be shown that σ is symmetric.

2.1.2 Material Laws

The system we have now is still underdetermined. The missing equations are given by material laws. Because we are in linear elasticity, we first use a linear interrelation between stress and strain, called **Hook's Law**:

$$\sigma = C\epsilon\ ,$$

where ϵ is the strain, depending on u via the geometrical relations. C is the material tensor of the elastic coefficients $C_{i,j,k,l}$. By the symmetry of σ and the use of istotrop materials and material objectivity law the different entries can be reduced from 81 entries to 2. These two constants are called Lamé constants λ and μ of a material.
The representation of σ follows from Hook's law

$$\begin{aligned}\sigma &= C\epsilon \\ &= C_{ijkl}\epsilon\ ,\end{aligned}$$

and, taking only isotropic and homogeneous materials, it leads to the relations

$$\sigma = (\lambda(\delta_{ij}\delta_{kl} + \mu(\delta_{ik}\delta_{jl} + \delta_{il}\delta_{jk}))\epsilon(u)\ ,$$

$$\sigma = \lambda tr(\epsilon(u))I + 2\mu\epsilon(u)\ , \tag{2.1}$$

where δ_{ij} is the Kronecker Delta. Materials with this properties are called St.Vernant-Kirchhoff materials.

In practise they are often expressed in terms of the elasticity module ("Young Modulus") and the lateral contraction ("Poisson ratio") as they

are frequently used in mechanics:

$$E := \frac{\mu(3\lambda + 2\mu)}{\lambda + \mu},$$
$$\nu := \frac{\lambda}{2(\lambda + \mu)}.$$

Imagine a rod, which is pulled in one direction: E is the ratio of the stress in that direction to the relative change of length. ν is the negative ratio of the relative change of the diameter of the rope to the relative change of the length of the rope.
By this formulas it is obvious that $\lambda, \mu > 0$ respectively $E > 0$ and $0 < \nu < \frac{1}{2}$ have to be fulfilled.

2.1.3 Linear Quasistatic Elastisity Model

Summarizing the previous results leads to the model for linear elastisticity:

Balance of Momentum	$-div\ \sigma = F_V$ in $\Omega \times [0, T]$
Balance of Angular Momentum	$\sigma = \sigma^T$
Hook's Law	$\sigma = C\epsilon$
Geometrical Relations (Linerized Strain)	$\epsilon(u) = \frac{1}{2}(\nabla u + (\nabla u)^T)$
Boundary Conditions	$u = u_D$ on Γ_D and
	$\sigma_n = g$ on Γ_N

2.2 Elastoplasticity Model

Now irreversible deformations are introduced, which are called plastic deformation. This plastic deformation does not disappear if the load is removed, because the load was high enough, that in some parts of the material the chemical lattice structure was destroyed and shifted. The new chemical lattice can only be shifted back under the complementary load. Thus, some modifications of our model have to be done. The material law is changing. Let's plot the stress-strain relation of an elastoplastic material.

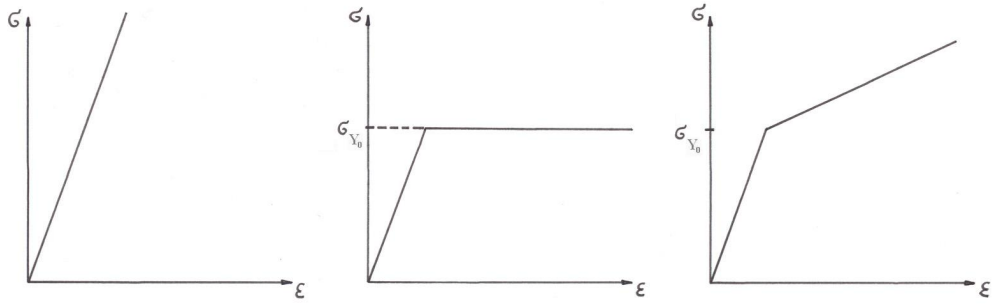

Figure 2.1: Abstract stress-strain relations: elastic behaviour (left), perfect plastic behaviour (middle) and plastic behaviour with hardening (right)

On the left side, we can see the behaviour of elastic materials, in the middle, perfect plastic materials, and, on the right side, a typical section of the strain stress relation of a material like steel. Plastic deformation can occur at some place where some stress reaches the critical value, the yield stress σ_{Y_0}. From that point on the stress-strain relation is not linear any more and the slope of the curve decreases. Practically this means that the deformation increases disproportionally fast. In the elastic case loading and unloading does not influence the stress-strain relation. In the case of plastic materials we have to deal with the hysteresis, this means that by unloading the elastic behaviour appears earlier and in the next loading step more force is needed to get the same effect as in the loading step before. That effect, the need of more force in the next loading step, is called hardening of the material. Considering the case of perfect plasticity no hardening arsises, because the slope of the curve in the plastic behaviour zone is 0. The hardening parameter is proportional to the slope of the stress-strain curve in the plastic part.
This thesis only takes isotropic hardening in account, this means hardening only with a scalar hardening parameter and not a tensor.

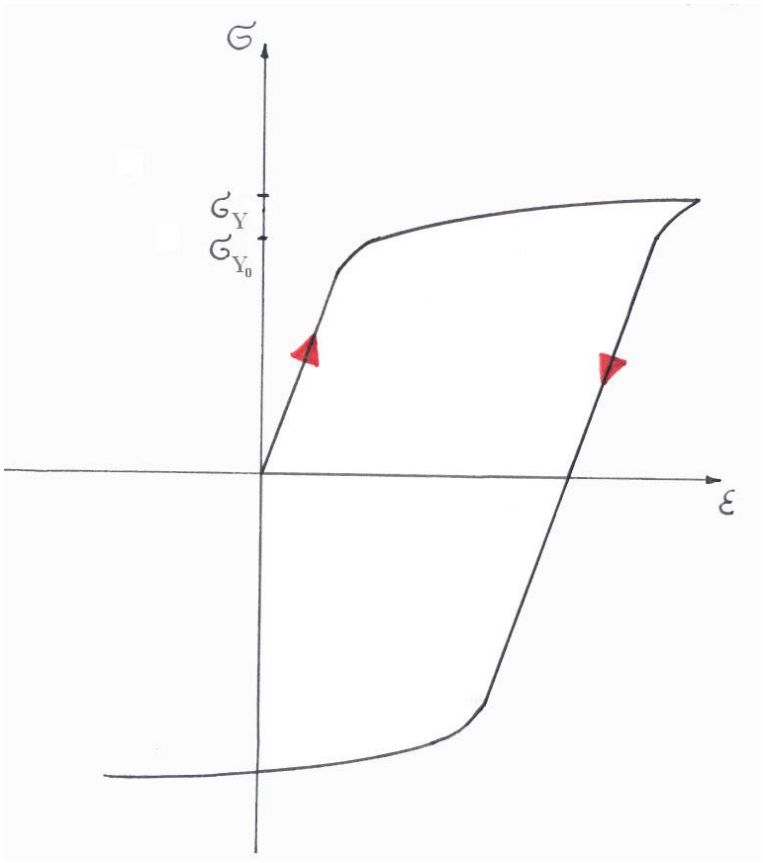

Figure 2.2: Iterated loading and undloading

As we can see in the Figure 2.2 the strain can be splitted into two parts, elastic and plastic. As far as we do not pay attention on the area where elastic and plastic behaviour overlaps, the splitting is the sum of two linear function.

$$\epsilon = e + p\,,$$

where e is the elastic part of the strain and p is the plastic one. So, Hook's Law can be formulated only for the elastic part, in the following way

$$\sigma = C(\epsilon - p).$$

The plastic flow p is mostly defined incremental where

$$\dot{p} = 0 \text{ if } \begin{cases} \sigma \in (-\sigma_Y, \sigma_Y)\,, \\ \sigma = \sigma_Y \text{ and } \dot{\sigma} \leq 0\,, \\ \sigma = -\sigma_Y \text{ and } \dot{\sigma} \geq 0\,, \end{cases}$$

and

$$\dot{p} = \frac{\dot{\sigma}}{H} \text{ if } \begin{cases} \sigma = \sigma_Y \text{ and } \dot{\sigma} > 0\,, \\ \sigma = -\sigma_Y \text{ and } \dot{\sigma} < 0\,, \end{cases}$$

where H is the "modulus of hardening".

2.2.1 Maximum plastic work principle

In order to decide if the stress-strain relation is elastic or plastic we use a yield function $\bar{\phi}$. Many different definitions have been proposed, but the most common method is to use the von Mises yield function. The hardening parameter is defined as α so that

$$\bar{\phi}(\sigma, \alpha) = \| \, dev \, \sigma \, \|_F - \sigma_Y(1 + \alpha H) \qquad \text{if } \alpha \geq 0.$$

The set of admissible stresses K can be defined by

$$K = \{\sigma \mid \bar{\phi}(\sigma, \alpha) \leq 0\}\,,$$

or by the dissipation functional φ

$$\varphi(\sigma, \alpha) = \begin{cases} 0 & \text{if } \bar{\phi}(\sigma, \alpha) \leq 0\,, \\ \infty & \text{if } \bar{\phi}(\sigma, \alpha) > 0\,. \end{cases}$$

Proposition 2.1 *Under the assumption that no hardening occurs:*
Let σ be a given stress with $\bar{\phi}(\sigma, 0) = 0$, $\dot{p}$ be the plastic flow and τ be a admissible stress. Then the prinicple of maximum work holds and

$$\sigma : \dot{p} \geq \tau : \dot{p}\,.$$

Introducing a hardening parameter and and the law changes to the Prantl-Reuss normality law. Let(τ, β) be all admissible pairs of stress and hardening parameters, φ is the so-called dissipation functional, defined as

$$\varphi(p, \alpha) = \begin{cases} \sigma_Y \, \| \, p \, \|_F & tr(p) = 0 \text{ and } (\alpha + H\sigma_Y) \leq 0\,. \\ \infty & \text{otherwise.} \end{cases}$$

Then the inequality

$$\dot{p}(\tau - \sigma) - \dot{\alpha}(\beta - \alpha) \leq \varphi(\tau, \beta) - \varphi(\sigma, \alpha)$$

holds, see also [11].

2.2.2 Elastoplastic Model

Until now we have not mentioned the time dependence of the problem, involved by setting initial conditions the model is complete.

$$\begin{aligned} u(x,0) &= u_0(x)\,, \\ \sigma(x,0) &= \sigma_0(x)\,. \end{aligned}$$

Now we put all the equations together to the elastoplastic model:
Let us now summarize the relations which completely describe the elastoplastic behaviour:

Balance of Momentum:	$-div\ \sigma = F_V$ in $\Omega \times [0,T]$ *(equilibrium of forces)*
Balance of of Angular Momentum:	$\sigma = \sigma^T$ *(equilibrium of momentum)*
Hook's Law:	$\sigma = C(\epsilon - p)$
Linerized Strain-Displacement relations:	$\epsilon(u) = \frac{1}{2}(\nabla u + (\nabla u)^T)$ *(geometrical relations)*
Boundary Conditions:	$u = u_D$ on Γ_D and $\sigma_n = g$ on Γ_N
Initial Conditions:	$p(x,0) = p_0(x)$ $\alpha(x,0) = \alpha_0(x)$
Admissibility:	$\varphi(\sigma,\alpha) < \infty$
Plastic Flow:	$\dot{p} : (\tau - \sigma) - \dot{\alpha} : (\beta - \alpha) \leq \varphi(\tau,\beta) - \varphi(\sigma,\alpha)$ $\forall(\tau,\beta)$ admissible

For the variational formulation we need the dual formulation of the plastic flow. The reformulations are made with the theorems of the convex analysis results of the first chapter

$$\begin{aligned} \dot{p} : (\tau - \sigma) - \dot{\alpha} : (\beta - \alpha) &\leq \varphi(\tau,\beta) - \varphi(\sigma,\alpha)\,, \\ \langle (\dot{p}, -\dot{\alpha}), (\tau,\beta) - (\sigma,\alpha) \rangle &\leq \varphi(\tau,\beta) - \varphi(\sigma,\alpha)\,, \end{aligned}$$

$\forall(\tau,\beta)$ admissible. By using Equation 1.2 it can be rewritten with the subdifferential

$$\begin{aligned} (\dot{p}, -\dot{\alpha}) &\in \partial\varphi(\sigma,\alpha) \\ (\sigma,\alpha) &\in \partial\varphi^*(\dot{p}, -\dot{\alpha}) \\ \sigma : (q - \dot{p}) + \alpha : (\gamma + \dot{\alpha}) &\leq \varphi^*(q,\gamma) - \varphi^*(\dot{p}, -\dot{\alpha}) \qquad \forall(q,\gamma) \end{aligned}$$

2.3 Plain Stress Model

Our problem settings in the numerical experiments always take in account geometries, which have in one dimension a very small expansion in comparision to the other two ones. This geometric property leads to numerical problems by using 3D finite elements. The plain stress model provides a method to discretize the geometry only in 2D, which reduces the computing time dramatically and avoids numerical problems caused by the volume elements. We have to take into account that all force only can be applied in the plane of the large dimensions (like f in Figure 2.3). Hence, in that approach all stresses that appear between the large dimensions and the small one are set to 0, because they are much smaller in relation to the others.

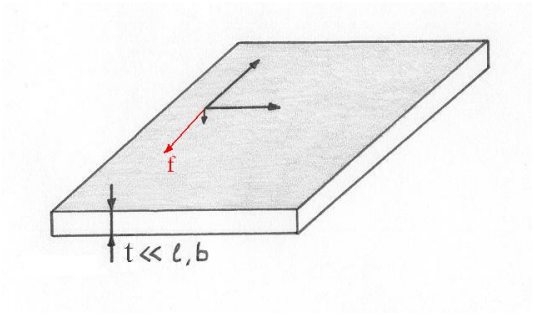

Figure 2.3: Typical geometry for a plain stress model

The simplification will only be shown for the elastic case, the priciple for the elastoplastic case is basically the same.
Let's consider σ and ϵ in its vector representation. Remember that the two tensors are symmetric. By the use of St.Vernant-Kirchhoff materials and the pair $\{E, \nu\}$ for Hook's Law, $\sigma = C\epsilon = \lambda tr(\epsilon(u))I + 2\mu\epsilon$ transforms to:

$$\begin{pmatrix} \sigma_{11} \\ \sigma_{22} \\ \sigma_{33} \\ \sigma_{12} \\ \sigma_{13} \\ \sigma_{23} \end{pmatrix} = \frac{E}{(1+\nu)(1-2\nu)} \begin{pmatrix} 1-\nu & \nu & \nu & 0 & 0 & 0 \\ \nu & 1-\nu & \nu & 0 & 0 & 0 \\ \nu & \nu & 1-\nu & 0 & 0 & 0 \\ 0 & 0 & 0 & 1-2\nu & 0 & 0 \\ 0 & 0 & 0 & 0 & 1-2\nu & 0 \\ 0 & 0 & 0 & 0 & 0 & 1-2\nu \end{pmatrix} \begin{pmatrix} \epsilon_{11} \\ \epsilon_{22} \\ \epsilon_{33} \\ \epsilon_{12} \\ \epsilon_{13} \\ \epsilon_{23} \end{pmatrix}$$

Since we mentioned before the plain stress model only considers stresses in those two directions where the dimensions are not too small. Therefore

$$\sigma_{13} = \sigma_{23} = \sigma_{33} = 0$$
$$\sigma_{31} = \sigma_{32} = 0,$$

the system reduces to

$$\begin{pmatrix} \sigma_{11} \\ \sigma_{22} \\ \sigma_{12} \end{pmatrix} = \frac{E}{(1-\nu^2)} \begin{pmatrix} 1 & \nu & 0 \\ \nu & & 0 \\ 0 & 0 & 1-\nu \end{pmatrix} \begin{pmatrix} \epsilon_{11} \\ \epsilon_{22} \\ \epsilon_{12} \end{pmatrix}$$

and the relation $\epsilon_{33} = -\frac{\nu}{1-\nu}(\epsilon_{11} + \epsilon_{22})$ results from the material law (2.1). For the numerical experiments the plain stress model or alternative the plain strain model can be implemented.

Chapter 3

Variational Formulation and Time Discretization

The variational or weak formulation is the starting point for the finite element discretization. The describing equations are

$$\begin{aligned} -div\ \sigma = F_V \qquad & \text{in } \Omega \times [0,T] && \text{(equilibrium equation),} \\ \sigma = C(\epsilon - p) & && \text{(Hook's law),} \\ \epsilon = \frac{1}{2}(\nabla u + (\nabla u)^T) & && \text{(geometric relation).} \end{aligned}$$

The first step is always the multiplication with the test function. The space of the test function V_0 is defined as

$$V_0 = [H_0^1(\Omega)]^d = \{v = (v_i) \mid v_i \in H_0^1(\Omega)\ \forall i \in \{1, 2, ...d\}\}$$

where

$$H_0^1(\Omega) = \{w \in H^1(\Omega) \mid w = 0 \text{ on } \Gamma_D\}$$

and d is the dimension of the domain.
To derive the variational form we take the equilibrium equation multiply by a test function and intergrate over the domain Ω

$$\begin{aligned} -\int_\Omega div\ \sigma.v\ dx &= \int_\Omega F_V.v\ dx \\ -\int_\Omega (div\ (\sigma.v) - \sigma : \nabla v)\ dx &= \int_\Omega F_V.v\ dx \end{aligned}$$

Using the symmetry of σ we arrive at the equation

$$\int_\Omega \sigma : \epsilon(v)\ dx - \int_\Omega div\ (\sigma v)\ dx \ = \ \int_\Omega F_V.v\ dx,$$

and by the Gauss theorem it can be rewritten as

$$\begin{aligned} \int_\Omega \sigma : \epsilon(v)\ dx - \int_{\partial\Omega} (\sigma v).n\ ds &= \int_\Omega F_V.v\ dx, \\ \int_\Omega \sigma : \epsilon(v)\ dx &= \int_\Omega F_V.v\ dx + \int_{\partial\Omega} (\sigma n)\cdot v\ ds, \\ \int_\Omega C(\epsilon(u)-p) : \epsilon(v)\ dx &= \int_\Omega F_V.v\ dx + \int_{\Gamma_N} g.v\ ds. \end{aligned}$$

3.1 Dual Formulation

While we are dealing with a plastic problem our variational form is a variational inequality with the plastic flow condition as part of the system. By using the dual formulation of the inequality we only have to integrate over the domain Ω, because the test functions are all admissible pairs of stress and hardening parameter $(q, \gamma) \in W$. The test space W is defined as follows:

$$W = [L_2(\Omega)]^{d\times d}_{symm} \times L_2(\Omega)$$

The dual formulation as calculated in Section 2.2.2 can be rewritten in form of a variational inequality:

$$\int_\Omega C(\epsilon(u)-p) : (q-\dot{p}) + \alpha : (\gamma + \dot{\alpha})\ dx \ \leq \ \int_\Omega \varphi^*(q,\gamma) - \varphi^*(\dot{p}, -\dot{\alpha})\ dx$$

that hold for all test functions $(q, v) \in W$.

3.2 Variational Form of the Problem

Find $(u, p, \alpha) \in V_D \times W$ such that

$$\int_\Omega C(\epsilon(u)-p) : \epsilon(v)\ dx \ = \ \int_\Omega F_V(t).v\ dx + \int_{\Gamma_N} g(t).v\ ds \qquad \forall v \in V_0$$

and

$$\int_\Omega C(\epsilon(u)-p) \;:\; (q-\dot{p})+\alpha : (\gamma+\dot{\alpha})\,dx \leq \int_\Omega \varphi^*(q,\gamma)-\varphi^*(\dot{p},-\dot{\alpha})\,dx \qquad \forall (q,\gamma)\in W$$

is fulfilled.

3.3 Time Discretization

We discretize in time by the backward Euler scheme, i.e., we replace the derivative of p with respect to time by the backward difference quotient with time step size τ. The same scheme is applied to α. This gives the finite difference approxing terms:

$$\dot{p} \;\approx\; \frac{p^{l+1}-p^l}{\tau}$$

and

$$\dot{\alpha} \;\approx\; \frac{\alpha^{l+1}-\alpha^l}{\tau}\,.$$

The problem can be reformulated by regarding this time discretization scheme as: Find $(u^{l+1},p^{l+1},\alpha^{l+1})\in V_D\times W$ such that the identity

$$\int_\Omega C(\epsilon(u^{l+1})-p^{l+1}):\epsilon(v)\,dx \;=\; \int_\Omega F_V\cdot\vec{v}\,dx+\int_{\Gamma_N} g\cdot\vec{v}\,ds \qquad (3.1)$$

is fulfilled for all $v\in V_0$ and the inequality

$$\int_\Omega C(\epsilon(u^{l+1})-p^{l+1}) \;:\; (q-\frac{p^{l+1}-p^l}{\tau})+\alpha^{l+1} : (\gamma+\frac{\alpha^{l+1}-\alpha^l}{\tau})\,dx \leq \int_\Omega \varphi^*(q,\gamma)-\varphi^*(\frac{p^{l+1}-p^l}{\tau},-\frac{\alpha^{l+1}-\alpha^l}{\tau})\,dx$$

holds for all $\forall(q,\gamma)\in W$.

3.4 Minimization Form

Our first goal is to rewrite the model by its energy minimization problem. As it is shown in [1], the problem should be reformulated first in terms of the bilinear form a, the linear term L and some functional j.
The first equation is clear, because except v no other test function influences the equation. So let's have a look at the inequality. We can rewrite it so that

$$\int_\Omega C(\epsilon(u^{l+1}) - p^{l+1}) : (\tau q - p^{l+1} + p^l) + \alpha^{l+1} : (\gamma\tau + \alpha^{l+1} - \alpha^l)\, dx \\ \leq \tau \int_\Omega \varphi^*(q,\gamma) - \varphi^*(\frac{p^{l+1} - p^l}{\tau}, -\frac{\alpha^{l+1} - \alpha^l}{\tau})\, dx \quad (3.2)$$

holds for all $(q, \gamma) \in W$.
Let us rewrite the Equations 3.1 and 3.2 in an abstract way.

$$a_1(x, x-y) = L(x-y) \qquad \forall y \in Y \quad (3.3)$$
$$a_2(x, x-y) \leq j(x) - j(y) \qquad \forall y \in Y \quad (3.4)$$

On that system we can easily apply the machinery of proofing existence and uniqueness. The crucial point is to find the right setting of the test functions.
Since looking for $(u^{l+1}, p^{l+1}, \alpha^{l+1}) \in V_D \times W$ the state variable x which should be calculated as $x = (x_1, x_2, x_3)$ with the setting $x_1 = u^{l+1}, x_2 = p^{l+1}$ and $x_3 = \alpha^{l+1}$. The test function $y = (y_1, y_2, y_3)$ consists of the components

$$\begin{aligned} y_1 &= u^{l+1} - v \\ y_2 &= \tau q + p^l \\ y_3 &= -\gamma\tau + \alpha^l \end{aligned}$$

The required functionals $a_1(x,y), a_2(x,y), L(x), j(x)$ are defined as

$$\begin{aligned} a_1(x,y) &= \int_\Omega C(\epsilon(x_1) - x_2) : \epsilon(y_1)\, dx \\ a_2(x,y) &= \int_\Omega -C(\epsilon(x_1) - x_2) : y_2 + x_3 y_3\, dx \\ L(x) &= \int_\Omega F_V \cdot x_1\, dx + \int_{\Gamma_N} g \cdot x_1\, ds \\ j(x) &= \tau \int_\Omega \varphi^*(\frac{x_2 - p^l}{\tau}, \frac{-x_3 + \alpha^l}{\tau})\, dx \end{aligned}$$

Together with the definition of $a(x,y) = a_1(x,y) + a_2(x,y)$ the summation of 3.3 and 3.4 leads to the inequality

$$a(x, x-y) \leq L(x-y) + j(x) - j(y) \qquad \forall y \in Y. \tag{3.5}$$

Notice, that if x solves 3.5, then x solves 3.3 and 3.4 also.
As it can be shown, the solution of the inequality 3.5 is equivalent to the minimization of an energy functional, i.e.

$$E(x) = \min_{z \in V_D \times W} E(z)$$

where E is defined as

$$E(z) = \frac{1}{2} a(z,z) + j(z) - L(z)$$

or more explicity,

$$\begin{aligned} E(x) &= \frac{1}{2}[\int_\Omega C(\epsilon(x_1) - x_2) : \epsilon(x_1)\, dx \\ &+ \int_\Omega -C(\epsilon(x_1) - x_2) : x_2 + x_3^2\, dx] \\ &+ \tau \int_\Omega \varphi^*(\frac{x_2 - p^l}{\tau}, \frac{-x_3 + \alpha^l}{\tau})\, dx \\ &- \int_\Omega F_V \cdot x_1\, dx - \int_{\partial\Omega} g \cdot x_1\, ds \end{aligned}$$

Thus, the problem, in term of minimization is the following:

Find $(u^{l+1}, p^{l+1}, \alpha^{l+1}) \in V_D \times W$ such that

$$f(u^{l+1}, p^{l+1}, \alpha^{l+1}) = \inf_{(u,p,\alpha) \in V_D \times W} f(u,p,\alpha)\ ,$$

where

$$\begin{aligned} f(u,p,\alpha) &:= \frac{1}{2} \int_\Omega C(\epsilon(u) - p) : (\epsilon(u) - p) + \alpha\, dx \\ &+ \tau \int_\Omega \varphi^*(\frac{p - p^l}{\tau}, -\frac{\alpha - \alpha^l}{\tau})\, dx \\ &- \int_\Omega F_V \cdot u\, dx - \int_{\partial\Omega} g \cdot u\, ds\ . \end{aligned}$$

is the minimization functional.

As it was mentioned above there are different hardening laws. In this thesis isotropic hardening is considered, where the functional φ^* reads

$$\varphi^*(p,\alpha) = \begin{cases} \sigma_Y \parallel p \parallel_F & tr(p) = 0 \text{ and } (\alpha + H\sigma_Y) \leq 0 \\ \infty & \text{otherwise} \end{cases}$$

Also the hardening parameter of the next time step α^{l+1} can be expressed in term of the parameter in the previous time step and the slope of the stress-strain curve. This relation can be formulated mathematical as

$$\alpha^{l+1} = \alpha^l + \sigma_Y H \parallel p \parallel_F$$

p is defined incrementally so replace p by $\frac{p^{l+1}-p^l}{\tau}$. Now ending up with the implemented problem

Find $(u^{l+1}, p^{l+1}) \in V_D \times [L_2(\Omega)]^{3\times 3}_{symm}$ such that

$$\hat{f}(u^{l+1}, p^{l+1}) = \inf_{(u,p)\in V_D \times W} \hat{f}(u,p)$$

where

$$\begin{aligned} \hat{f}(u,p) &= \frac{1}{2}\int_\Omega C(\epsilon(u)-p) : (\epsilon(u)-p) && (3.6)\\ &+ (\alpha^l + \sigma_Y H \parallel p - p^l \parallel_F)^2 dx && (3.7)\\ &+ \int_\Omega \sigma_Y \parallel p - p^l \parallel_F \; dx && (3.8)\\ &- \int_\Omega F_V \cdot u \; dx - \int_{\partial\Omega} g \cdot u \; ds && (3.9) \end{aligned}$$

is the minimization functional.

3.5 Newton Method

As we know from optimization theory, the first derivative of an minimization problem is 0 if the minimum of the function is reached.
We know that p is a funtional

$$p^{l+1} = \frac{\max(\parallel devC(\epsilon(u^{l+1}) - p^l) \parallel_F - \sigma_Y(1+\alpha^l H), 0)\; dev\; C(\epsilon(u^{l+1}) - p^l)}{(2\mu + \sigma_Y^2 H^2) \parallel devC(\epsilon(u^{l+1}) - p^l) \parallel_F} + p^l \;,$$

so we can understand f as a functional only depending on u as follows:

$$\begin{aligned} f(u^{l+1}) &= \frac{1}{2}\int_\Omega C(\epsilon(u^{l+1}) - p^{l+1}(\epsilon(u^{l+1}))) : (\epsilon(u^{l+1}) - p^{l+1}(\epsilon(u^{l+1}))) \\ &+ (\alpha^l + \tau\sigma_Y H \parallel p^{l+1}(\epsilon(u^{l+1})) - p^l \parallel_F)^2 dx \\ &+ \int_\Omega \sigma_Y \parallel p^{l+1}(\epsilon(u^{l+1})) - p^l \parallel_F \; dx \\ &- \int_\Omega F_V \cdot u^{l+1}\, dx - \int_{\Gamma_N} g \cdot u^{l+1}\, ds\,. \end{aligned}$$

The first (Gâuteaux) derivative of this functional f exists and is given by

$$\begin{aligned} Df(u^{l+1}, v) &= \int_\Omega C(\epsilon(u^{l+1}) - p^{l+1}(\epsilon(u^{l+1}))) : \epsilon(v)\, dx \qquad (3.10) \\ &- \int_\Omega F_V \cdot u^{l+1}\, dx - \int_{\Gamma_N} g \cdot u^{l+1}\, ds\,. \qquad (3.11) \\ & \qquad (3.12) \end{aligned}$$

In 1965 J.J.Moreau proved, that f is Frchet differentable and thus Equation (3.10) is the Fréchet derivative of f.
If also the second derivative of f (in some sense) exists, we can use Newton's method to solve the problem. The general purpose of a Newton method is to find the root of the functional by the iterating scheme

$$x_{n+1} = x_n - F'(x_n)^{-1} F(x_n),$$

where x_n is u and the function F is the Gâuteaux derivative of the energy functional $Df((u^{l+1}, v)$ and $F'(x_n)$ is the second derivative.
Thus, the minimization problem can be solved by a Newton-like method. The second derivative does not exist classically, but can be replaced by a slanting function the Fréchet derivative.

Definition 3.1 *(slant differentiability pointwise)*
Let $U \subset \mathbb{R}^N$ be an open subset and $x \in U$. A function $F : U \to Y$ is said to be slantly differentiable at x *if there exist*

1. *mappings $F^\circ : U \to L(X, Y)$ and $r : X \to Y$ with $\lim_{h\to 0} \frac{\|r(h)\|}{\|h\|} = 0$ such, that*
$$F(x + h) = F(x) + F^\circ(x + h)\, h + r(h)$$
holds for all $h \in X$ satisfying $(x + h) \in U$, and

2. *constants* $\delta > 0$ *and* $C > 0$ *such that for all* $h \in X$ *with* $\| h \| < \delta$ *there holds*

$$\| F^\circ(x+h) \| := \sup_{y \in X \setminus \{0\}} \frac{\| F^\circ(x+h)\, y \|}{\| y \|} \leq C\,.$$

We say, that $F^\circ(x)$ *is a* slanting function for F at x.

$D^2 f$ is a slanty derivative F° and so we can modify the newton method to

$$x_{n+1} = x_n - F^\circ(x_n)^{-1} F(x_n). \tag{3.13}$$

The next theorem will guarantee us the convergence of the iteration scheme (3.13).

Theorem 3.1 *Let* $U \subset X$ *be an open subset, and* $F : U \to Y$ *be a slantly differentiable function with a slanting function* $F^\circ : U \to Ł(X, Y)$. *We suppose, that* $x^* \in U$ *is a solution to the nonlinear problem* $F(x) = 0$. *If* $F^\circ(x)$ *is non-singular for all* $x \in U$ *and* $\| F^\circ(x)^{-1} : x \in U \|$ *is bounded, then the Newton-like iteration*

$$x^{j+1} = x^j - F^\circ(x^j)^{-1} F(x^j) \tag{3.14}$$

converges super-linearly to x^*, *provided that* $\| x^0 - x^* \|$ *is sufficiently small.*

Proof: See [4].

For more details, theory and implementation see [9].

Chapter 4

Discretization and Implementation

In Chapter 3 the time discretization was already done. For computing a solution also the space discretization of the elastioplastic problem has to be done.
In order to do the space discretization we have to decompose the given domain Ω into a mesh of finite elements δ_r.
The set of triangles is given by $\Im_h = \{\delta_r : r \in \mathbb{R}_h\}$, where h is the discretization parameter, which defines the fineness of the mesh. $\mathbb{R}_h$ is the set of global element numbers $\{1, ..., R_h\}$, where R_h is the total number of elements. The global node numbering is given by $\bar{\omega_h} = \{1, ..., \bar{N}_h\}$ where $\bar{N}_h = N_h + \partial N_h$ is the total number of the nodes, inner nodes and Dirichet boundary nodes.

4.1 Mapping

The local node numbering is important for the mapping principle of the FEM: Give a local definition of the basis functions via the shape functions (= basis functions $|_{\delta_r}$), which are defined by mapping the shape functions of the master element to the element $\delta_r \in \Im_h$.

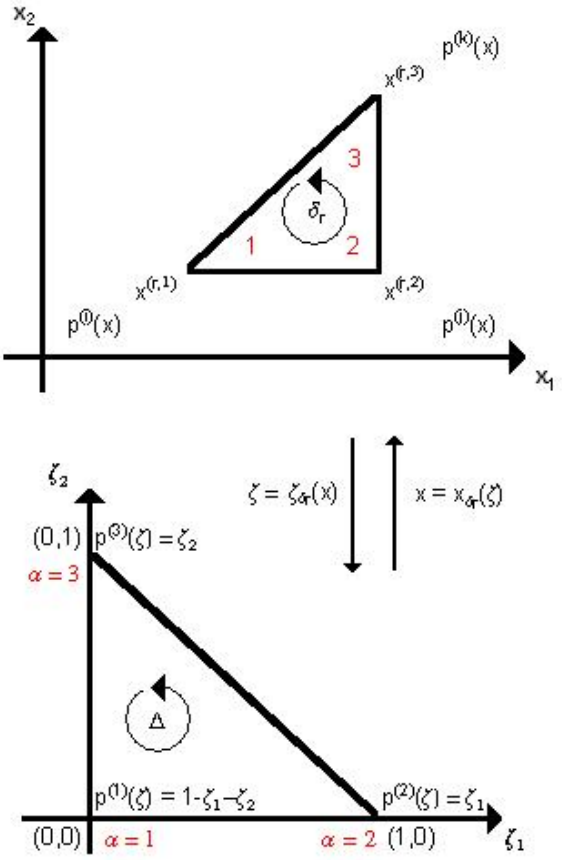

Figure 4.1: Mapping of each triangle with the basis function (see the bottom picture) on the reference triangle.

The affine linear mapping reads

$$x \;=\; x_{\delta_r}(\zeta) = J_{\delta_r} \cdot \zeta + x^{(i)},$$

where $J_{\delta_r} = \frac{\partial x}{\partial \zeta}$ denotes the Jacobian of the mapping $x = x_{\delta_r}(\zeta)$.
There we get

$$x = \begin{pmatrix} x_1 \\ x_2 \end{pmatrix} = \begin{pmatrix} x_{1j} - x_{1i} & x_{1k} - x_{1i} \\ x_{2j} - x_{2i} & x_{2k} - x_{2i} \end{pmatrix} \cdot \begin{pmatrix} \zeta_1 \\ \zeta_2 \end{pmatrix} + \begin{pmatrix} x_{1i} \\ x_{2i} \end{pmatrix}.$$

Now the basis functions are defined

$$p^{(i)}(x) = \begin{cases} p^{(r,\alpha)}(x) & x \in \bar{\delta}_r, r \in B_i, \\ 0 & \text{otherwise,} \end{cases}$$

with $B_i = \{r \in \mathbb{R}_h : x^{(i)} \in \bar{\delta}_r\}$ and $p^{(r,\alpha)}(x) = p^{(\alpha)}(\zeta_{\delta_r}(x))$ with $x \in \bar{\delta}_r$,where $p^{(\alpha)}(\zeta_{\delta_r}(x))$ is the shape function of the master element (see Figure 4.1). So the nodal basis functions fulfil the relation

$$p^{(i)}(x^{(j)}) = \delta_{ij} \qquad \forall i, j \in \bar{\omega_h}.$$

This choice of p is called Courant basis functions.

4.2 Extrapolation of the starting value

It is well-known that the choice of a proper starting value for Newton-like methods is very important for the convergence. To save computing time and guarantee fast convergence we can use the solutions from the former time step and the next coarser mesh. After extrapolation we reach a good starting value for the Newton method, which minimizes the energy functional as it was described above.
The extrapolation formula reads

$$u_{t+1}^{l+1} = u_t^{l+1} + I_l^{l+1}(u_{t+1}^l - u_t^l),$$

where l is the level of refinements and t is the time step. I_l^{l+1} is the FEM-Interpolation operator, which maps the difference of the solution on the next coarser grid level.
In Figure 4.2 the system of calculation is shown and it is obvious to see that only the solution at the first time step and the solution on the coarsest mesh have to be evaluated with the classical approach as it is done in [9].

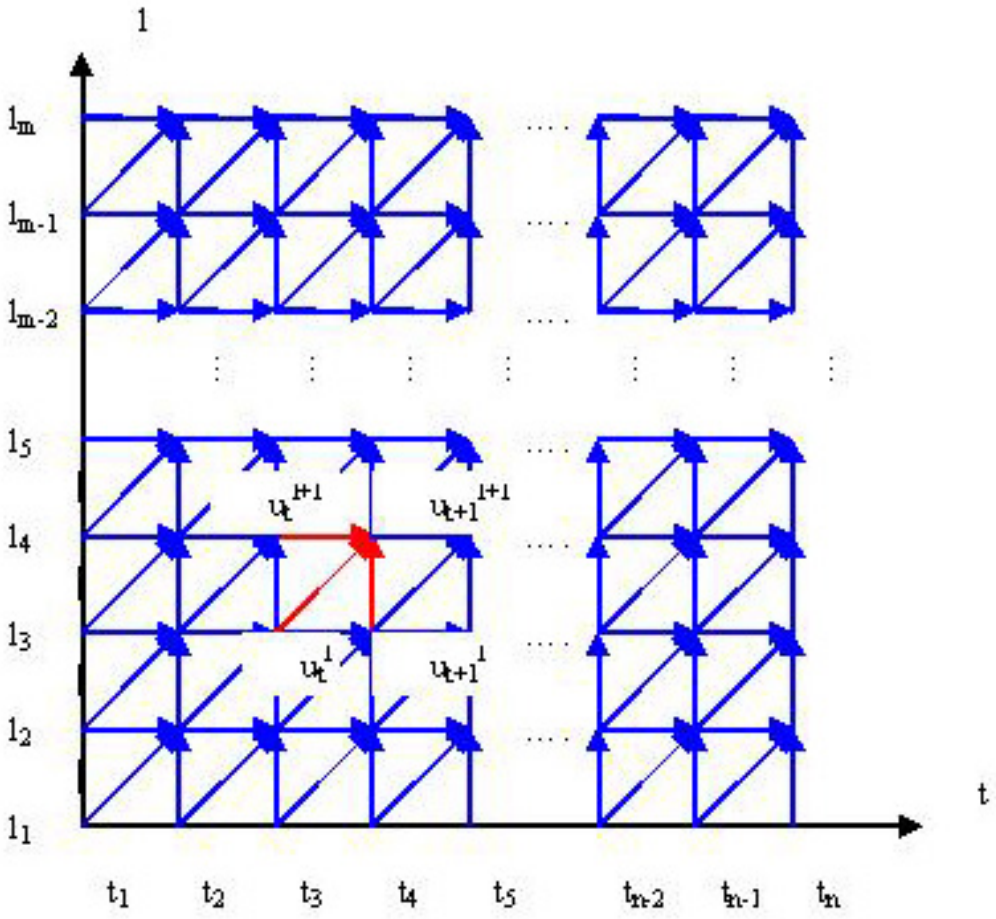

Figure 4.2: Using the solution in the three points we get a good approximation for a good starting value of the solution u. It is obvious that this scheme only works if the level $l \geq 1$ and the time step $n > 0$

Algorithm 4.1 *Extrapolation*

if ($t > t_0$ *and Newton method converges in the last time step)*
  if (at least one refinement is done)
    u=Extrapolation$(u(refinement, t), u(refinement, t-1))$
  else
    $u_t = u_{t-1}$
  end
else
  if (at least one refinement is done)
    $u = u_{coarser\ grid}$ *if node exists in coarser grid and 0 else*
  end
end

The basic purpose of the next algorithm is to calculate the extrapolation formula of the solution as it is given in Algorithm 4.1. The finite element discretization consists of triangles with Courant basis functions. We also assume that new nodes are placed in the middle of an edge, that is why the extrapolation of the solution can be done in the following way:

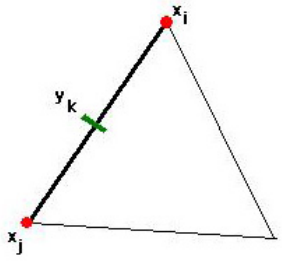

Figure 4.3: Refinement structures caused by bisecting the edges

The nodes of the coarser grid are denoted by x_i and the nodes of the actual grid by y_k. y_k is the new node between x_i and x_j. An interpolation of the displacement u is then done by

$$u_{y_k} = \frac{1}{2}(u_{x_i} + u_{x_j}).$$

Algorithm 4.2 *Extrapolation of the solution*

%extrapolate the solution from the next coarser grid
$u(y_k) = u_{x_k}$ if the node exists in coarser grid and $\frac{1}{2}(u_{x_i} + u_{x_j})$ else
$\Rightarrow u(l,t)$
% extrapolate the solution from the previous time step
search if node exists in the former grid
if(not found) then do recursive
search for the corresponding basis nodes of the new node
check if basis nodes exist
end
reconstruct the extrapolated u $\Rightarrow u(l,t-1)$
the solution to the coarser grid in the previous time step is extrapolated as in the acual time step $\Rightarrow u(l-1,t-1)$
% extrapolation formula
$u(l,t) = u(l,t-1) + (u(l-1,t) - u(l-1,t-1))$

The algorithm is fast enough as the searching structure for the new nodes is quite good. In our case the time step is small enough, so there are only few new nodes which do not exists in the previous time step.

4.3 Extrapolating the Plastic Strain

By minimizing with respect to p^{l+1} and fixed u^{l+1} our work leads to a recursive definition of p as it is shown in [1]

$$p^{l+1} = \frac{\max(\parallel devA \parallel_F - \vartheta, 0)\ dev\ A}{(2\mu + \sigma_Y^2 H^2) \parallel devA \parallel_F} + p^l$$

where

$$\begin{aligned} A &= C(\epsilon(u^{l+1}) - p^l) \\ \vartheta &= \sigma_Y(1 + \alpha^l H) \end{aligned}$$

This is the reason why all can be expressed in terms of u: $p = p(\epsilon(u^{l+1}))$. The formula above will be used to compute the new plastic strain in the time step $l+1$ using the plastic strain of the previous time step modified by the suspected slope of the stress-strain curve. We have to remember

the nested grid structure explained in the introduction chapter to keep in mind that the coarse mesh in every time step is the same, but the refinements leads to different meshes in every time step. Concerning the plastic strain is constant on each element, p can also be concentrated in any point inside the element. Here the center of mass is choosen. Let us denote the individual plastic strains of each element by p_i. Looking at Figure 4.3, we can see that not every element existing in the time step l also exists in the time step $l + 1$.

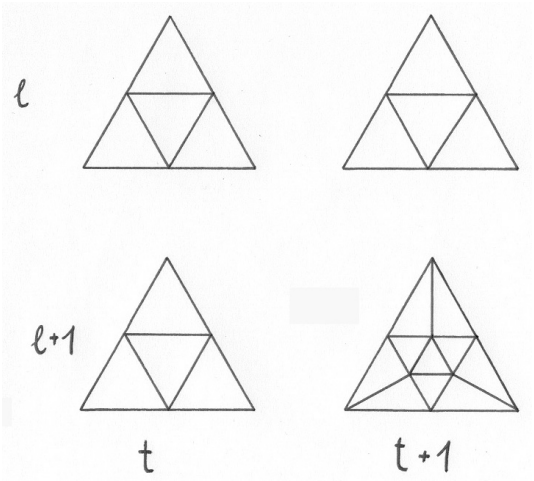

Figure 4.4: Nested grid structure for the extrapolation

Reference Triangle Transformation

To decide if a point is in a special triangle or not, the point as well as the triangle $\{p_1, p_2, p_3\}$ have to be transformed to the reference configuration. Afterwards, while knowing the reference triangle has the vertices $p_1' = (0, 0), p_2' = (0, 1), p_3' = (1, 0)$, the implemented Matlab program checks if the point is inside the triangle or not. Mathematically expressed:

Proposition 4.1 *The transformation of points from the general mesh to the mesh of the reference triangle of a special triangle T in the general mesh is the following: Let be J of two entries x and y. p is the point which we want to transform and p' the corresponing point in the reference mesh of the triangle T. Then there holds*

$$
\begin{aligned}
J &= \begin{pmatrix} p_2.x - p_1.x \\ p_3.x - p_1.x \\ p_2.y - p_1.y \\ p_3.y - p_1.y \end{pmatrix}, \\
p' &= J^{-1}(p - p1).
\end{aligned}
$$

The point p' is inside the triangle if the next 3 conditions hold:

- $p'.x \geq 0$,
- $p'.y \geq 0$,
- $p'.x + p'.y \leq 1$.

So we have to do extrapolation. A fast method is to look in which element of the mesh in the former time step p_i is located. The plastic strain located in the recovered element is the new plastic strain in the new time step modified as discussed above.

For the decision if extrapolation should be done or not we use the same algorithm as above with one modification. At the first time step or if the solution in the previous time step do not converges then we do nothing.
The extrapolation of the plastic strain is done in a different way, because the plastic strain defined over one triangle as a constant. For simplification we choose one point in the triangle and there the plastic strain values are settled.
Since we always start with the same grid in every time step we only have to save the history of the refining the basis triangles to get a quick extrapolation.

Algorithm 4.3 *Extrapolation of the plastic strain*

for each triangle i
B:=basistriangle of triangle i
browse through all triangles lying in B in the previous time step
check if coordinates of $p_i(t)$ *lies inside the triangle* $\Rightarrow p_i = p_i(t-1)$
end

In the section of the numerical results we can see that this extrapolation is quite good and fast enough.

4.4 Analysis of the Nested Iteration Algorithm

It is important to know how good the approximation of the solution with the nested iteration algortihm and the extrapolation is. As it is shown in [14] for stronger assumptions the iteration number will be universal for each mesh size h and every time step t.

Theorem 4.1 *We assume $u \in H^2(\Omega)$ at all time steps t, and the convergence of the incremental method as the approximation $E_h(u) = \inf_{v_h \in V_h} \parallel u - v_h \parallel_{1,\Omega} \leq a_{1,2} h \parallel u \parallel_{2,\Omega}$ holds.*
The convergence rates ρ_e and ρ_p of the iteration processes with the iteration solver operator for the elastic problem S_q^0 and for the plastic problem S_q^n where q is the index of h and $n \in 1, \ldots, N-1$ where N is the number of time steps. The iteration solver operator should be independent of the number level in h and the time steps N, also of q and n the actual position of the pair (level,time step) and the operators have to be less than 1 in the corresponding norm. The first convergence rate is fixed as $\rho_1 \in (0,1)$ and for all q the inequality $h_{q-1} \leq b h_q$ holds. In the case where only refinements, which bisect the side length of the triangle are allowed, b is equal to 2.
Then univeral (independent), positive iteration numbers exists such that the approximations

$$\begin{aligned} \mid u_{t,q}^n - v_{t,q}^n \mid_V &\leq \alpha(\Delta t + h_q) \\ \mid \sigma_{t,q} - \tau_{t,q}^n \mid_S + \mid p_{t,q} - \pi_{t,q}^n \mid_\Pi &\leq \alpha(\Delta t + h_q) \end{aligned}$$

with $\alpha > 0$ where u, σ, p the exact solutions and v, τ, π the approximate solutions of the nested iteration scheme.

Proof:
Only a short view on the proof is given, the exact one is done in [14]

- Show global H^2-regularity: By the so-called A-properties for our problem with isotropic hardening it follows that only one solution

to the problem can exist. Furthermore regularity statements for the increment of u, σ and p hold.

- Next have a look on the convergence of u and σ

- After proofing the assumptions consider $u^n_{t,q}$ as a fix point of the iteration solver operator

- Assume for $n = 0$ and $q = 1$ the approximation above holds and do
  - Induction with respect to q at time $n = 0$
  - Induction with respect to n at level $q = 1$
  - Diagonal induction from the pair$(q - 1, n - 1)$ to (q, n)

Chapter 5

Numerical Results

The nested iteration algorithm with the extrapolation of u, p and α was implemented in Matlab, version 7.2.0.294 (R2006a), under Linux. The calculations were done with a laptop model ACER TravelMate 8000 with a CPU of 1.7 GHz and 1024 MB RAM. The program was tested by three different examples under different loading regimes, namely linear loading and cyclic loading.
The new method is compared with the standard approach used in [7].
For more information about the residuals of the individual time steps or the plastic zone and the yield pictures, we enclosed a CD in the back.
Sometimes the Newton-like method does not converge (marked by - in the tables), but if newton damping will be used or the step size be adjusted the convergence will be reached.

5.1 L-Shape Problem

The L-shape domain is frequently used in literature for simulations. The problem is defined on the geometry in Figure 5.1.
On the boundery we set time dependent non-homogeneous Dirichlet boundery condition in polar coordinates r, θ

$$\begin{aligned} u_r(r,\theta) &= \frac{1}{2\mu} r^\alpha \left[-(\alpha+1)\cos((\alpha+1)\,\theta) + (C_2-(\alpha+1))C_1\cos((\alpha-1)\,\theta)\right], \\ u_\theta(r,\theta) &= \frac{1}{2\mu} r^\alpha \left[(\alpha+1)\sin((\alpha+1)\,\theta) + (C_2+(\alpha-1))C_1\sin((\alpha-1)\,\theta)\right]. \end{aligned}$$

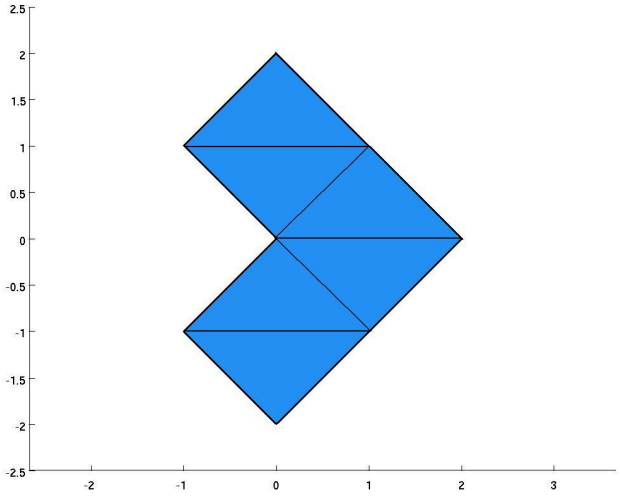

Figure 5.1: The geometry of the L-shape domain and the coarse mesh

where the deformation of the boundery is given by

$$u(t) = g(t) * (u_r * cos\theta - u_t * sin\theta, u_r * sin\theta + u_t * cos\theta) \tag{5.1}$$

The following settings are choosen for the calculation:

- material parameters: $E = 1e5, \nu = 0.3, H = 1, \sigma_Y = 2.2$
- magnification for displaying: $3e3$
- direct matlab solver used
- Newton termination criterion: $\epsilon = 1e - 12$
- no Newton damping factors are used
- refinement levels: 6 (all adaptive)
- time steps:
  - $t \in [0.1, 1.2]$ with step size 0.02 in the linear case where $g(t) = t$
  - $t \in [0.1, 1.5]$ with step size 0.02 in the cyclic case where $g(t) = \sin(\pi * t)$

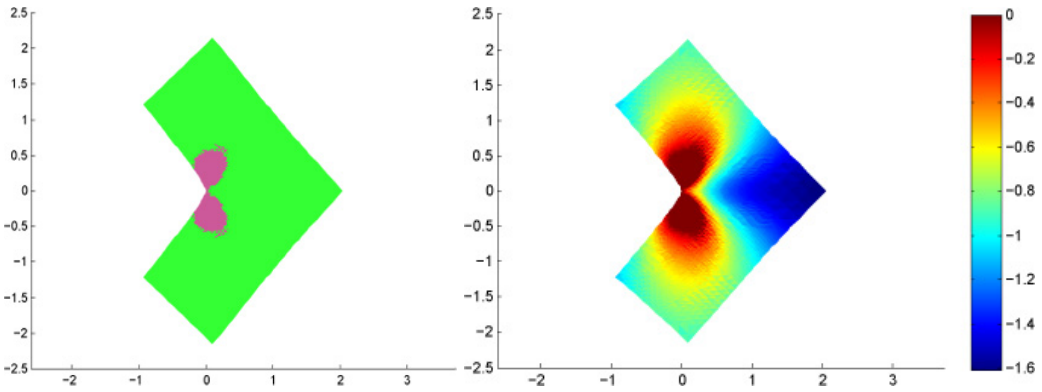

Figure 5.2: Left plastic zones, right picture yield stress under a linear loading regime

Let us take one time step in every loading case, for example 0.38 to illustrate the results. The program creates for every time step a pictures of the plastic zones and of the yield stress in the considered area. The plastic area is coloured pink while the elastic regions are green.

5.1.1 Linear loading

The count of Newton steps until reaching the termination criterion is shown in Table 5.1.Unfortunately the program of [7] can only refine uniform if more than one time step is required. So we take 5 uniform refinements levels to compare the two algorithm. In principle we can that the Newton steps are at both methods hardly the same. However, we can mentioned that the program works for a more general case (different meshes).

5.1.2 Cyclic loading

In Table 5.2 count of Newton steps until reaching the termination criterion on level 5 are given. For comparison the number of Newton steps which the program of [7] takes is given in brackets.
In Table 5.3 we use a mesh generated as 6 adaptive refinements. In comparison to Table 5.2 the steps are hardly the same.

time	steps	time	steps	time	steps
0.1	5 (5)	0.6	6 (6)	1.1	5 (5)
0.12	5 (5)	0.62	6 (5)	1.12	5 (5)
0.14	5 (5)	0.64	6 (6)	1.14	5 (5)
0.16	6 (6)	0.66	7 (6)	1.16	5 (6)
0.18	6 (5)	0.68	7 (6)	1.18	6 (5)
0.2	6 (5)	0.7	7 (5)	1.2	6 (5)
0.22	6 (5)	0.72	6 (5)		
0.24	6 (5)	0.74	6 (6)		
0.26	6 (6)	0.76	6 (5)		
0.28	6 (5)	0.78	6 (5)		
0.3	6 (5)	0.8	6 (5)		
0.32	7 (6)	0.82	6 (5)		
0.34	6 (6)	0.84	6 (6)		
0.36	6 (6)	0.86	6 (5)		
0.38	6 (5)	0.88	6 (5)		
0.4	6 (6)	0.9	6 (5)		
0.42	6 (6)	0.92	6 (5)		
0.44	6 (5)	0.94	6 (4)		
0.46	6 (6)	0.96	3 (2)		
0.48	6 (6)	0.98	2 (2)		
0.5	6 (6)	1.00	- (2)		
0.52	6 (6)	1.02	2 (2)		
0.54	6 (6)	1.04	2 (2)		
0.56	7 (5)	1.06	5 (4)		
0.58	6 (6)	1.08	5 (5)		

Table 5.1: Newton steps for the problem L-shape under the linear loading regime

time	steps	time	steps	time	steps
0.1	5 (5)	0.6	6 (6)	1.1	5 (5)
0.12	5 (5)	0.62	6 (5)	1.12	5 (5)
0.14	5 (5)	0.64	7 (6)	1.14	5 (5)
0.16	6 (6)	0.66	7 (6)	1.16	6 (6)
0.18	6 (5)	0.68	7 (6)	1.18	6 (5)
0.2	6 (5)	0.7	7 (5)	1.2	6 (5)
0.22	6 (5)	0.72	6 (5)	1.22	6 (5)
0.24	6 (5)	0.74	6 (6)	1.24	6 (5)
0.26	6 (6)	0.76	6 (5)	1.26	6 (6)
0.28	6 (5)	0.78	6 (5)	1.28	6 (5)
0.3	6 (5)	0.8	6 (5)	1.3	6 (5)
0.32	7 (6)	0.82	6 (5)	1.32	7 (6)
0.34	6 (6)	0.84	6 (6)	1.34	6 (6)
0.36	6 (6)	0.86	6 (5)	1.36	6 (6)
0.38	6 (5)	0.88	6 (5)	1.38	6 (5)
0.4	6 (6)	0.9	6 (5)	1.4	6 (6)
0.42	6 (6)	0.92	6 (5)	1.42	6 (6)
0.44	6 (5)	0.94	5 (4)	1.44	6 (5)
0.46	6 (6)	0.96	3 (2)	1.46	6 (6)
0.48	6 (6)	0.98	2 (2)	1.48	6 (6)
0.5	6 (6)	1.00	2 (2)	1.5	6 (6)
0.52	6 (6)	1.02	2 (2)		
0.54	6 (6)	1.04	2 (2)		
0.56	7 (5)	1.06	5 (4)		
0.58	6 (6)	1.08	5 (5)		

Table 5.2: Newton steps for the problem L-shape under the cyclic loading regime

time	steps	time	steps	time	steps
0.1	6	0.6	7	1.1	5
0.12	6	0.62	6	1.12	6
0.14	6	0.64	6	1.14	6
0.16	6	0.66	7	1.16	6
0.18	6	0.68	6	1.18	6
0.2	7	0.7	7	1.2	7
0.22	6	0.72	7	1.22	6
0.24	6	0.74	7	1.24	6
0.26	6	0.76	6	1.26	6
0.28	7	0.78	6	1.28	7
0.3	6	0.8	7	1.3	6
0.32	6	0.82	6	1.32	6
0.34	7	0.84	7	1.34	7
0.36	6	0.86	6	1.36	6
0.38	6	0.88	6	1.38	6
0.4	7	0.9	6	1.4	7
0.42	7	0.92	6	1.42	7
0.44	7	0.94	6	1.44	7
0.46	7	0.96	5	1.46	7
0.48	7	0.98	3	1.48	7
0.5	7	1.00	2	1.5	7
0.52	7	1.02	2		
0.54	7	1.04	5		
0.56	7	1.06	5		
0.58	7	1.08	5		

Table 5.3: Newton steps for the problem L-shape under the cyclic loading regime with adaptive refinements

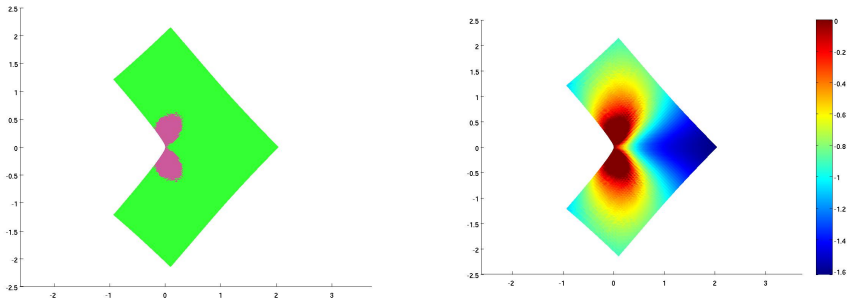

Figure 5.3: Left plastic zones, right picture yield stress under a cyclic loading regime

5.2 Wrench Problem

The wrench problem simulates a wrench with a screw, which is fixed in its position (see Figure 5.2). The applied force should models the human force pushing the wrench. The geometry is shown in the Figure 5.2. The boundery is a full Neumann boundery exept on the contact faces between wrench and screw, there we assume a Dirichlet boundery part.

The coarse mesh consists of 40 elements and 34 nodes. The following settings are choosen for the calculation:

- material parameters: $E = 2e8, \nu = 0.3, H = 0.001, \sigma_Y = 2e6$
- magnification for displaying: 10
- direct matlab solver used
- Newton termination criterion: $1e - 12$
- Newton damping factors are used
  (max. 3 inner iteration with damping factor 0.2)
- refinement levels: 5 (first uniform and then 4 times adaptive)
- time steps:
  - $t \in [0.1, 1.2]$ with step size 0.02 in the linear case where $g(t) = \bar{g}t$

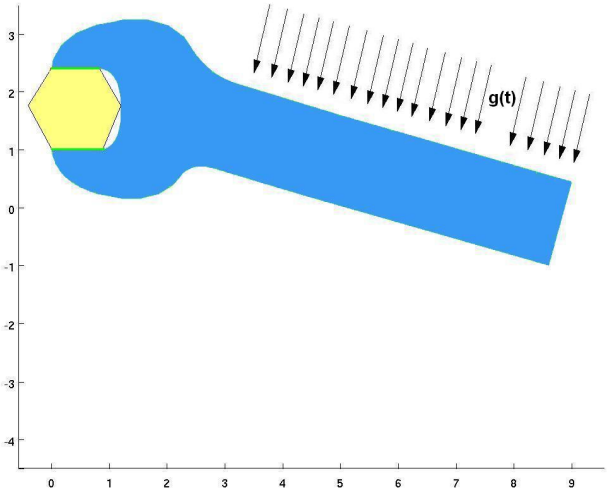

Figure 5.4: The geometry of the wrench and the applied force, everywhere the screw attends the wrench the boundary is fixed

- $t \in [0.1, 1.5]$ with step size 0.02 in the cyclic case where $g(t) = \bar{g}\sin(\phi t)$

Let us take one time step in every loading case, for example 0.38 to illustrate the results. The program creates for every time step a pictures of the plastic zones and of the yield stress in the considered are. The plastic area is coloured pink while the elastic regions are green.

5.2.1 Linear loading

In Table 5.4 the count of Newton steps is shown until reaching the termination criterion on level 4. For comparison the number of Newton steps which the program of [7] takes is given in brackets.

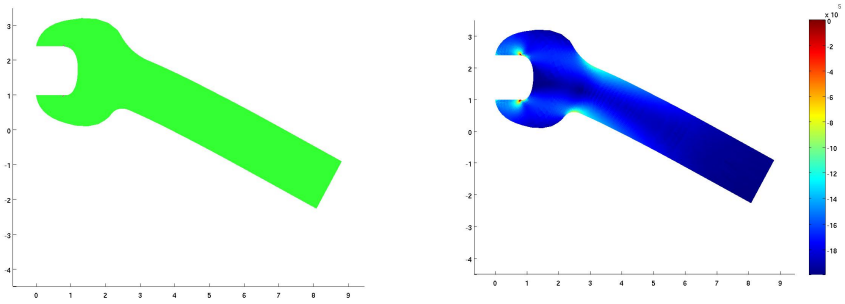

Figure 5.5: Left plastic zones, right picture yield stress under a linear loading regime

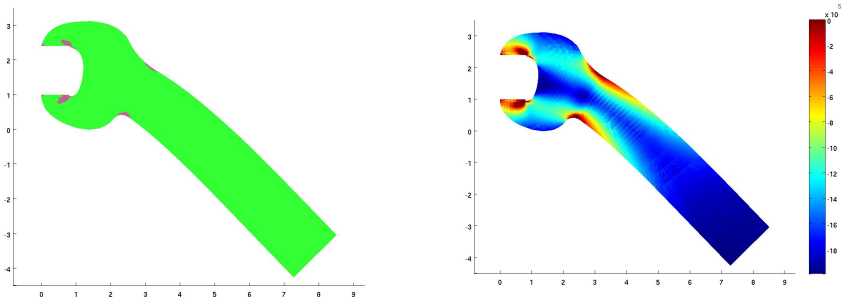

Figure 5.6: Left plastic zones, right picture yield stress under a cyclic loading regime

5.2.2 Cyclic loading

In Table 5.5 the count of Newton steps is shown until reaching the termination criterion on level 4. The numbers in brackets are the Newton steps which the program of [7] takes to calculate the same solution.

time	steps	time	steps	time	steps
0.1	2 (2)	0.6	6 (6)	1.1	9 (6)
0.12	2 (2)	0.62	6 (6)	1.12	11(7)
0.14	2 (2)	0.64	6 (6)	1.14	11(7)
0.16	2 (2)	0.66	6 (6)	1.16	12(8)
0.18	2 (2)	0.68	6 (6)	1.18	13(8)
0.2	2 (2)	0.7	6 (6)	1.2	14(7)
0.22	2 (2)	0.72	6 (7)		
0.24	2 (2)	0.74	6 (7)		
0.26	2 (2)	0.76	6 (6)		
0.28	2 (2)	0.78	6 (6)		
0.3	2 (2)	0.8	7 (7)		
0.32	2 (2)	0.82	7 (7)		
0.34	5 (5)	0.84	10(6)		
0.36	5 (5)	0.86	10(7)		
0.38	5 (5)	0.88	9 (6)		
0.4	5 (5)	0.9	8 (6)		
0.42	5 (5)	0.92	8 (6)		
0.44	5 (5)	0.94	8 (6)		
0.46	6 (5)	0.96	8 (6)		
0.48	5 (5)	0.98	8 (7)		
0.5	5 (6)	1.00	8 (7)		
0.52	5 (6)	1.02	8 (6)		
0.54	5 (6)	1.04	10(7)		
0.56	5 (6)	1.06	9 (6)		
0.58	5 (6)	1.08	9 (7)		

Table 5.4: Newton steps for the problem wrench under the linear loading regime

time	steps	time	steps	time	steps
0.1	2 (2)	0.6	8 (7)	1.1	2 (2)
0.12	5 (5)	0.62	8 (6)	1.12	5 (5)
0.14	5 (5)	0.64	8 (6)	1.14	5 (5)
0.16	6 (5)	0.66	6 (6)	1.16	6 (5)
0.18	6 (6)	0.68	6 (6)	1.18	6 (6)
0.2	7 (6)	0.7	7 (6)	1.2	7 (6)
0.22	6 (6)	0.72	6 (6)	1.22	6 (6)
0.24	7 (6)	0.74	6 (6)	1.24	7 (6)
0.26	6 (6)	0.76	6 (6)	1.26	6 (6)
0.28	6 (6)	0.78	6 (6)	1.28	6 (6)
0.3	7 (6)	0.8	6 (6)	1.3	7 (6)
0.32	10(6)	0.82	5 (6)	1.32	10(6)
0.34	11(6)	0.84	6 (5)	1.34	11(6)
0.36	8 (6)	0.86	5 (5)	1.36	8 (6)
0.38	8 (6)	0.88	5 (5)	1.38	8 (6)
0.4	8 (7)	0.9	4 (2)	1.4	8 (7)
0.42	8 (6)	0.92	2 (2)	1.42	8 (6)
0.44	8 (6)	0.94	2 (2)	1.44	8 (6)
0.46	8 (7)	0.96	2 (2)	1.46	8 (7)
0.48	8 (7)	0.98	2 (2)	1.48	8 (7)
0.5	9 (7)	1.00	2 (2)	1.5	9 (7)
0.52	8 (7)	1.02	2 (2)		
0.54	9 (7)	1.04	2 (2)		
0.56	9 (6)	1.06	2 (2)		
0.58	8 (6)	1.08	2 (2)		

Table 5.5: Newton steps for the problem wrench under the cyclic loading regime

Also in that example we can see that the iteration numbers are hardly the same. Table 5.6 shows the Newton steps if we choose 1 uniform mesh and 5 adaptive refinements

time	steps	time	steps	time	steps
0.1	1	0.6	12	1.1	5
0.12	6	0.62	10	1.12	6
0.14	7	0.64	11	1.14	7
0.16	7	0.66	11	1.16	7
0.18	8	0.68	12	1.18	8
0.2	8	0.7	10	1.2	8
0.22	8	0.72	10	1.22	8
0.24	9	0.74	10	1.24	9
0.26	9	0.76	9	1.26	9
0.28	10	0.78	9	1.28	10
0.3	10	0.8	11	1.3	10
0.32	10	0.82	8	1.32	10
0.34	10	0.84	8	1.34	10
0.36	10	0.86	8	1.36	10
0.38	10	0.88	6	1.38	10
0.4	10	0.9	6	1.4	10
0.42	14	0.92	5	1.42	14
0.44	13	0.94	3	1.44	13
0.46	14	0.96	2	1.46	14
0.48	14	0.98	2	1.48	14
0.5	14	1.00	3	1.5	14
0.52	14	1.02	2		
0.54	14	1.04	2		
0.56	13	1.06	2		
0.58	14	1.08	5		

Table 5.6: Newton steps for the problem wrench under the cyclic loading regime with adaptive refinements.

5.3 Plate with a Hole Problem

The plate with a hole problem simulates a steel plate with a hole placed at the middle of the plate. It is clear that the hole influences the behaviour of the material. Because of the symmetry only one quarter have to be calculated.

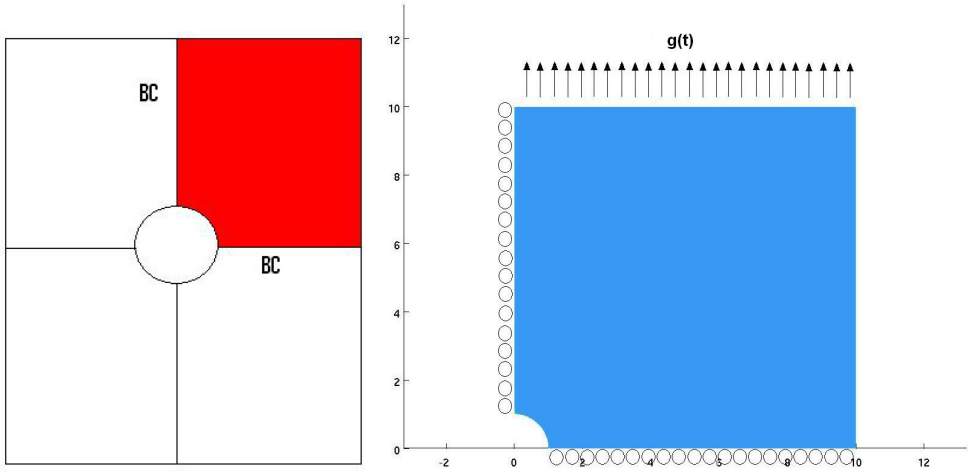

Figure 5.7: The total geometry of the plate with the hole problem is shown in the left figure. The implemented geometry with the symmetric boundary conditions is shown in the right figure with its applied force g(t)

The coarse mesh consists of of 132 elements and 225 nodes. The following settings are choosen for the calculation:

- material parameters: $E = 206900, \nu = 0.29, H = 0.5, \sigma_Y = 450\sqrt{\frac{2}{3}}$
- magnification for displaying: 50
- direct matlab solver used
- Newton termination criterion: $1e-12$
- no Newton damping factors are used

- refinement levels: 4 (the first refinement is done uniform, the others adaptive)
- time steps:
  - $t \in [0.1, 1.2]$ with step size 0.02 in the linear case where $g(t) = \bar{g}t$
  - $t \in [0.1, 1.5]$ with step size 0.02 in the cyclic case where $g(t) = \bar{g}\sin(\phi t)$

Let us take one time step in every loading case, for example 0.38 to illustrate the results. The program creates for every time step a pictures of the plastic zones and of the yield stress in the considered are. The plastic area is coloured pink while the elastic regions are green.

5.3.1 Linear loading

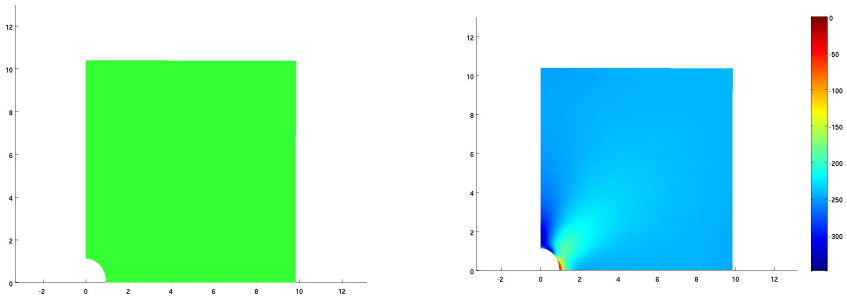

Figure 5.8: Left plastic zones, right picture yield stress under a linear loading regime

In Table 5.7 the count of Newton steps until reaching the termination criterion on level 3 is shown. The numbers in brackets are the Newton steps which the program of [7] takes to calculate the same solution.

time	steps	time	steps	time	steps
0.1	2 (2)	0.6	6 (5)	1.1	7 (6)
0.12	2 (2)	0.62	6 (5)	1.12	6 (5)
0.14	2 (2)	0.64	6 (5)	1.14	7 (5)
0.16	2 (2)	0.66	6 (5)	1.16	7 (6)
0.18	2 (2)	0.68	6 (5)	1.18	7 (6)
0.2	2 (2)	0.7	6 (5)	1.2	6 (5)
0.22	2 (2)	0.72	6 (5)		
0.24	2 (2)	0.74	6 (5)		
0.26	2 (2)	0.76	6 (5)		
0.28	2 (2)	0.78	6 (5)		
0.3	2 (2)	0.8	6 (5)		
0.32	2 (2)	0.82	6 (5)		
0.34	2 (2)	0.84	6 (6)		
0.36	2 (2)	0.86	6 (5)		
0.38	2 (2)	0.88	6 (5)		
0.4	5 (4)	0.9	6 (5)		
0.42	5 (5)	0.92	6 (6)		
0.44	5 (5)	0.94	6 (5)		
0.46	5 (5)	0.96	6 (6)		
0.48	6 (5)	0.98	6 (6)		
0.5	5 (5)	1.00	6 (5)		
0.52	5 (5)	1.02	6 (5)		
0.54	5 (5)	1.04	6 (5)		
0.56	6 (5)	1.06	7 (6)		
0.58	6 (5)	1.08	7 (6)		

Table 5.7: Newton steps for the problem plate with a hole under the linear loading regime

5.3.2 Cyclic loading

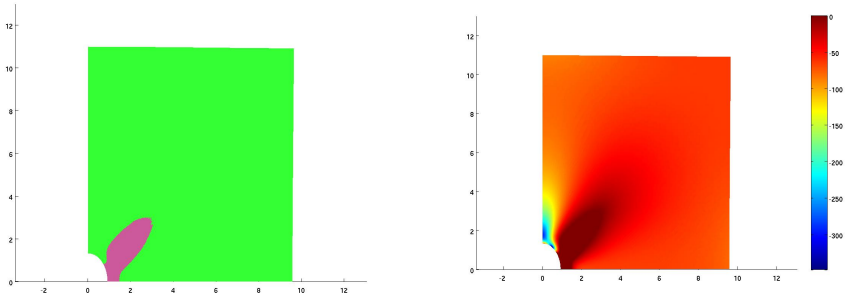

Figure 5.9: Left plastic zones, right picture yield stress under a cyclic loading regime

In Table 5.8 the count of Newton steps until reaching the termination criterion on level 3 is shown. For comparison the number of Newton steps which the program of [7] takes is given in brackets.
In Table 5.9 the results for one uniform refinement and 3 adaptive refinements are shown.

time	steps	time	steps	time	steps
0.1	2 (2)	0.6	6 (5)	1.1	2 (2)
0.12	2 (2)	0.62	6 (5)	1.12	2 (2)
0.14	5 (5)	0.64	6 (5)	1.14	5 (5)
0.16	5 (5)	0.66	6 (5)	1.16	5 (5)
0.18	5 (5)	0.68	6 (5)	1.18	5 (5)
0.2	6 (5)	0.7	6 (5)	1.2	6 (5)
0.22	7 (5)	0.72	6 (5)	1.22	7 (5)
0.24	6 (5)	0.74	6 (5)	1.24	6 (5)
0.26	6 (5)	0.76	6 (5)	1.26	6 (5)
0.28	6 (5)	0.78	7 (5)	1.28	6 (5)
0.3	6 (5)	0.8	6 (5)	1.3	6 (5)
0.32	6 (5)	0.82	6 (5)	1.32	6 (5)
0.34	6 (5)	0.84	6 (5)	1.34	6 (5)
0.36	6 (5)	0.86	6 (5)	1.36	6 (5)
0.38	6 (5)	0.88	4 (2)	1.38	6 (5)
0.4	6 (5)	0.9	2 (2)	1.4	6 (5)
0.42	6 (5)	0.92	2 (2)	1.42	6 (5)
0.44	6 (5)	0.94	2 (2)	1.44	6 (5)
0.46	6 (5)	0.96	2 (2)	1.46	6 (5)
0.48	6 (6)	0.98	2 (2)	1.48	6 (6)
0.5	6 (5)	1.00	2 (2)	1.5	6 (5)
0.52	6 (6)	1.02	2 (2)		
0.54	6 (5)	1.04	2 (2)		
0.56	6 (5)	1.06	2 (2)		
0.58	6 (5)	1.08	2 (2)		

Table 5.8: Newton steps for the problem plate with a hole under the cyclic loading regime

time	steps	time	steps	time	steps
0.1	2	0.6	6	1.1	2
0.12	2	0.62	7	1.12	2
0.14	5	0.64	6	1.14	5
0.16	6	0.66	6	1.16	6
0.18	5	0.68	6	1.18	5
0.2	6	0.7	7	1.2	6
0.22	7	0.72	7	1.22	7
0.24	7	0.74	7	1.24	7
0.26	7	0.76	7	1.26	7
0.28	7	0.78	7	1.28	7
0.3	6	0.8	6	1.3	6
0.32	6	0.82	7	1.32	6
0.34	6	0.84	6	1.34	6
0.36	6	0.86	6	1.36	6
0.38	6	0.88	4	1.38	6
0.4	6	0.9	2	1.4	6
0.42	6	0.92	2	1.42	6
0.44	6	0.94	2	1.44	6
0.46	6	0.96	2	1.46	6
0.48	6	0.98	2	1.48	6
0.5	7	1.00	2	1.5	7
0.52	6	1.02	2		
0.54	6	1.04	2		
0.56	6	1.06	2		
0.58	7	1.08	2		

Table 5.9: Newton steps for the problem plate with a hole under the cyclic loading regime and adaptive refinements

Chapter 6

Conclusion and Outlook

6.1 Conclusions

The main point of this thesis is that the nested iteration technique provides a time-independent number of Newton iterations, which can be calculated with some effort as it is described in the chapter on nested iteration technique. This technique is fast because of adaptive refinements in every step and level. This leads to a mangeable number of unknowns.

The needed extrapolation for the nested iterations is done on the one side on the nodes with the internode history for the displacements and on the other side by the element history for the plastic strain. If one wants to use different coarse mesh, only the first method can be adopted, the second has to be modified.

Since the numerical results have shown the iteration number for Newton in the linear loading regime is (nearly) independent of the spatial mesh and the time step. If convergence problems occur, they can be managed by introducing the Newton damping factor or taking a smaller time step size. This avoids Newton methods to diverge or oscillate between two values.

6.2 Outlook

A further approach to predict the interface of the elastic and the plastic region are boundary concentrated methods. Details can be looked up in [3],[12],[15] or [17].
To do boundary concentrated methods first we should first implement not only h-FEM but also p-FEM. With the so-called hp-FEM method the smooth parts would not be h refined, but the basis functions get a higher polynomial degree on each triangle. The interface, which is in our elasto-plastic problem the point of interest, will be refined to approximate the interface with highest possible accuracy, as in [5] is shown:

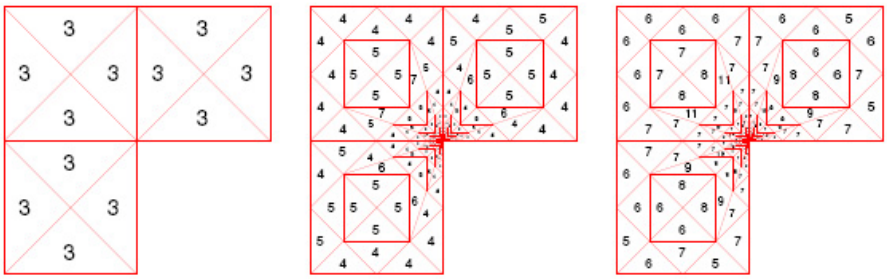

Figure 6.1: Boundary concentrated hp-FEM of the L-shape domain

For an further improvement of the method one should not only implement the hp-FEM, but also a prediction for the next time step should be formulated.
By combining the two techniques we can develop a fast and precise identifier for the interface. Think of a structure where the problem for few elements is solved and while refining the mesh by hp-FEM and extrapolating the starting values by nested iteration schemes the solution to the problem can be calculated very fast.
This result is the starting point for the boundary concentrated method. The predicted interface is the origin of the domain decomposition in plastic and elastic zones. In the elastic part of the domain the solution can be calculated quick because there occurs no nonlinearity from the plastic strain. The plastic part needs some more effort to calculate, but this is rather small for most of the applied loads and problems.
Since it is known from the analysis, the boundary concentrated method provides a optimal complexity of $O(N)$. The discretization error is also

only order $O(N)$ where N is the number of nodes on the boundary (interfaces). So a two-dimensional problem behaves under this conditions like a one-dimensional problem.

Appendix
List of Notation

d	$\in \{1, 2, 3\}$, space dimension
Ω	$\subset \mathbb{R}^d$, open bounded Lipschitz domain
Γ	$= \partial\Omega$, domain boundary
Γ_D	$\subset \Gamma$, Dirichlet boundary (prescribed displacements)
Γ_N	$\subset \Gamma$, Neumann boundary (prescribed surface tractions)
n	outer normal of Γ
σ	stress tensor
ε	elastic strain tensor
u	displacement
p	plastic strain tensor
α	hardening parameter
f	body or volume forces
u_D	prescribed displacement on Γ_D
g	prescribed surface tractions on Γ_N
λ	$\in \mathbb{R}^+$, "Lamé modulus", Lamé constant
μ	$\in \mathbb{R}^+$, "sheer modulus", Lamé constant
E	$\in \mathbb{R}^+$, "Young's modulus"
ν	$\in \left[0, \frac{1}{2}\right]$, "Poisson ratio"
δ_{ij}	"Kronecker delta"
C	$\in \mathbb{R}^{d\times d}_{d\times d}$ with $C_{ijkl} = \lambda\delta_{ij}\delta_{kl} + \mu(\delta_{ik}\delta_{jl} + \delta_{il}\delta_{jk})$, elasticity tensor
H	$\in \mathbb{R}^+$, "modulus of hardening"
σ_Y	$\in \mathbb{R}^+$, yield stress
φ	dissipation functional
ϕ	yield function
$\dot{f}$	$= \frac{\partial f}{\partial t}$, time derivative of a function f
∇f	$= \left(\frac{\partial f_i}{\partial x_j}\right)_{i,j}$, gradient of a (vector) function f
Δf	$= \sum_i \frac{\partial^2 f_i}{\partial^2 x_i}$, Laplace of a vector function f
Df	Fréchet Derivative of a function f
$\parallel A \parallel_F$	$:= \sqrt{\sum_{i,j} a_{ij}^2}$, Frobenius norm of a matrix A

Bibliography

[1] J. Alberty, C.Carstensen, and D. Zarrabi: *Adaptive numerical analysis in primal elastoplasticity with hardening*, Comput. Methods Appl. Mech. Eng. 171 (1999), no. 3-4, 175204

[2] S.S. Antman: *Nonlinear problems of elasticity*, Applied Mathematical Science, vol. 107, Springer, 1995.

[3] S. Beuchler, T. Eibner, U. Langer: *Primal and Dual Interface Concentrated Iterative Substructuring Methods*. Johann Radon Institute for Computational and Applied Matheamtics (RICAM), RICAM-Report 2007-07, 2007

[4] Xiaojun Chen, Zuhair Nashed, and Liqun Qi: *Smoothing methods and semismooth methods for nondifferentiable operator equations* SIAM Journal on Numerical Analysis 38(2000), no. 4, 12001216.

[5] T. Eibner: *Randkonzentrierte und adaptive hp-FEM*, PhD thesis, Technical University Chemnitz, 2006.

[6] I. Ekeland and R.Temam: *Convex analysis and variational problems*, Classics in Applied Mathematics, vol. 28, Society for Industrial and Applied Mathematics (SIAM), 1999, Unabridged, corrected republication of the 1976 original.

[7] P.G.Gruber: *Solution of Elastoplastic Problems based on Moreau-Yosida Theorem*, Johannes Kepler University Linz, 2006.

[8] P.G. Gruber and J. Valdman: *Newton-like solver for elastoplastic problems with hardening and its local super-Linear convergence*,Johannes Kepler University Linz, Special Research Program SFB F013 "Numerical and Symbolic Scientific Computing", SFB-Report 2007-06, Linz, 2007.

[9] P.G. Gruber and J. Valdman: *New numerical solver for elastoplastic problems based on the Moreau-Yosida theorem*. Johannes Kepler University Linz, Special Research Program SFB F013 "Numerical and Symbolic Scientific Computing", SFB-Report 2006-05, 2006.

[10] W. Hackbusch: *Multi-Grid Methods and Applications*, Heidelberg, Springer, 1985

[11] W.Han and B.D.Reddy: *Plasticity: Mathematical theory and numerical analysis*, Interdisciplinary Applied Mathematics, vol 9, Springer, 1999.

[12] B.N. Khoromskij, J.M. Melenk: *Boundary Concentrated Finite Element Methods*. SIAM J. Numer. Anal. 41 (2003), pp. 1-36

[13] J. Kienesberger: *Efficient Solution Algorithm for Elastoplastic Problems*. Phd thesis, SFB F013, Johannes Kepler University,Linz, 2007

[14] V.Korneev, U.Langer: *Approximate Solution of Plastic Flow Theory Problems*, Teubner Texte zur Mathematik, Band 69, Leipzig, 1984.

[15] R. Kornhuber, H Yserentant: *Multilevel Methods for Elliptic Problems on Domains not Resolved by the Coarse Grid*. D. E. Keyes and J. Xu (eds.) Proc. of the 7th Int. Conf. on Domain Decomposition Methods 1993. Providence, RI: AMS 1994. Pp. 49-60

[16] V.A.Lubarda and A.Hoger: *On the mechanics of solids with a growing mass*. Int. J. Solids Structures, Band 39, 2002.

[17] H. Yserentant: *Coarse grid spaces for domains with a complicated boundary*. Springer, Numerical Algorithms, Volume 21, Numbers 1-4, September 1999 , pp. 387-392(6)

Eidesstattliche Erklärung

Ich, Birgit Rauchenschwandtner, erkläre an Eides statt, dass ich die vorliegende Diplomarbeit selbstständig und ohne Hilfe verfasst, andere als die angegebenen Quellen und Hilfsmittel nicht benutzt bzw. die als wörtlich oder sinngemäß entnommenen Stellen als solche kenntlich gemacht habe.

Linz, Juli 2007

Birgit Rauchenschwandtner

Curriculum Vitae

Name:	Birgit Rauchenschwandtner
Nationality:	Austria
Date of Birth:	July 21, 1983
Place of Birth:	Salzburg, Austria

Education:

1989 - 1993	Volksschule (elementary school), Strawalchen
1993 - 1997	Hauptschule (secondary modern school), Strawalchen
1997 - 2002	HTL for electronics, Salzburg
2002 - 2005	Baccalaureat studies in Technical Mathematics, Johannes Kepler Universität Linz
2003 - 2006	Baccalaureat studies in Statistics, Johannes Kepler Universität Linz
2005 - 2007	Master studies in Industrial Mathematics, Johannes Kepler Universität Linz
2006 -	Master studies in Statistics, Johannes Kepler Universität Linz